ANNUAL SUMMARY

Atlantic Hurricane Season of 2008*

DANIEL P. BROWN, JOHN L. BEVEN, JAMES L. FRANKLIN, AND ERIC S. BLAKE

NOAA/NWS/NCEP, National Hurricane Center, Miami, Florida

(Manuscript received 27 July 2009, in final form 17 September 2009)

ABSTRACT

The 2008 Atlantic hurricane season is summarized and the year's tropical cyclones are described. Sixteen named storms formed in 2008. Of these, eight became hurricanes with five of them strengthening into major hurricanes (category 3 or higher on the Saffir–Simpson hurricane scale). There was also one tropical depression that did not attain tropical storm strength. These totals are above the long-term means of 11 named storms, 6 hurricanes, and 2 major hurricanes. The 2008 Atlantic basin tropical cyclones produced significant impacts from the Greater Antilles to the Turks and Caicos Islands as well as along portions of the U.S. Gulf Coast. Hurricanes Gustav, Ike, and Paloma hit Cuba, as did Tropical Storm Fay. Haiti was hit by Gustav and adversely affected by heavy rains from Fay, Ike, and Hanna. Paloma struck the Cayman Islands as a major hurricane, while Omar was a major hurricane when it passed near the northern Leeward Islands. Six consecutive cyclones hit the United States, including Hurricanes Dolly, Gustav, and Ike. The death toll from the Atlantic tropical cyclones is approximately 750.

A verification of National Hurricane Center official forecasts during 2008 is also presented. Official track forecasts set records for accuracy at all lead times from 12 to 120 h, and forecast skill was also at record levels for all lead times. Official intensity forecast errors in 2008 were below the previous 5-yr mean errors and set records at 72–120 h.

1. Introduction

Overall activity during the 2008 Atlantic season (Fig. 1 and Table 1) was above average. There were 16 tropical storms, of which 8 became hurricanes, including 5 major hurricanes [maximum 1-min winds of greater than 96 kt (1 kt = 0.5144 m s^{-1}) corresponding to category 3 or greater on the Saffir–Simpson hurricane scale; Saffir 1973; Simpson 1974]. These numbers are well above the long-term (1966–2007) averages of 11.2, 6.2, and 2.3, respectively. Typically most hurricane activity occurs between August and October; the 2008 season, however, featured major hurricane activity in every month from July to November. In terms of accumulated cyclone energy [(ACE; Bell et al. 2000); the sum of the squares of the maximum wind speed at 6-h intervals for (sub)tropical storms and hurricanes], activity in 2008 was about 167% of the long-term (1951–2000) median value of 87.5 × 10^4 kt^2.

The above-average activity observed in 2008 appears to have resulted from a combination of two factors. Although the 2007–08 La Niña dissipated early in the summer, the atmosphere in the Atlantic basin remained in a favorable configuration for enhanced tropical cyclone activity with a large area of lower-than-average vertical wind shear observed between 10° and 20°N (Fig. 2; Bell et al. 2009). In addition to the atmospheric conditions, sea surface temperatures (SSTs) in the tropical Atlantic Ocean were considerably above the long-term mean (Fig. 3). The SSTs were the fifth warmest since 1950 across the deep tropical Atlantic Ocean and Caribbean Sea.

Many of the 2008 Atlantic basin tropical cyclones affected land, resulting in significant impacts from the Greater Antilles to the Turks and Caicos Islands as well as on portions of the U.S. Gulf Coast. Tropical Storm Fay and Hurricanes Gustav, Ike, and Paloma made

* Supplemental information related to this paper is available at the Journals Online Web site: http://dx.doi.org/10.1175/2009MWR3174.s1.

Corresponding author address: Daniel P. Brown, National Hurricane Center, 11691 SW 17th St., Miami, FL 33165.
E-mail: daniel.p.brown@noaa.gov

DOI: 10.1175/2009MWR3174.1

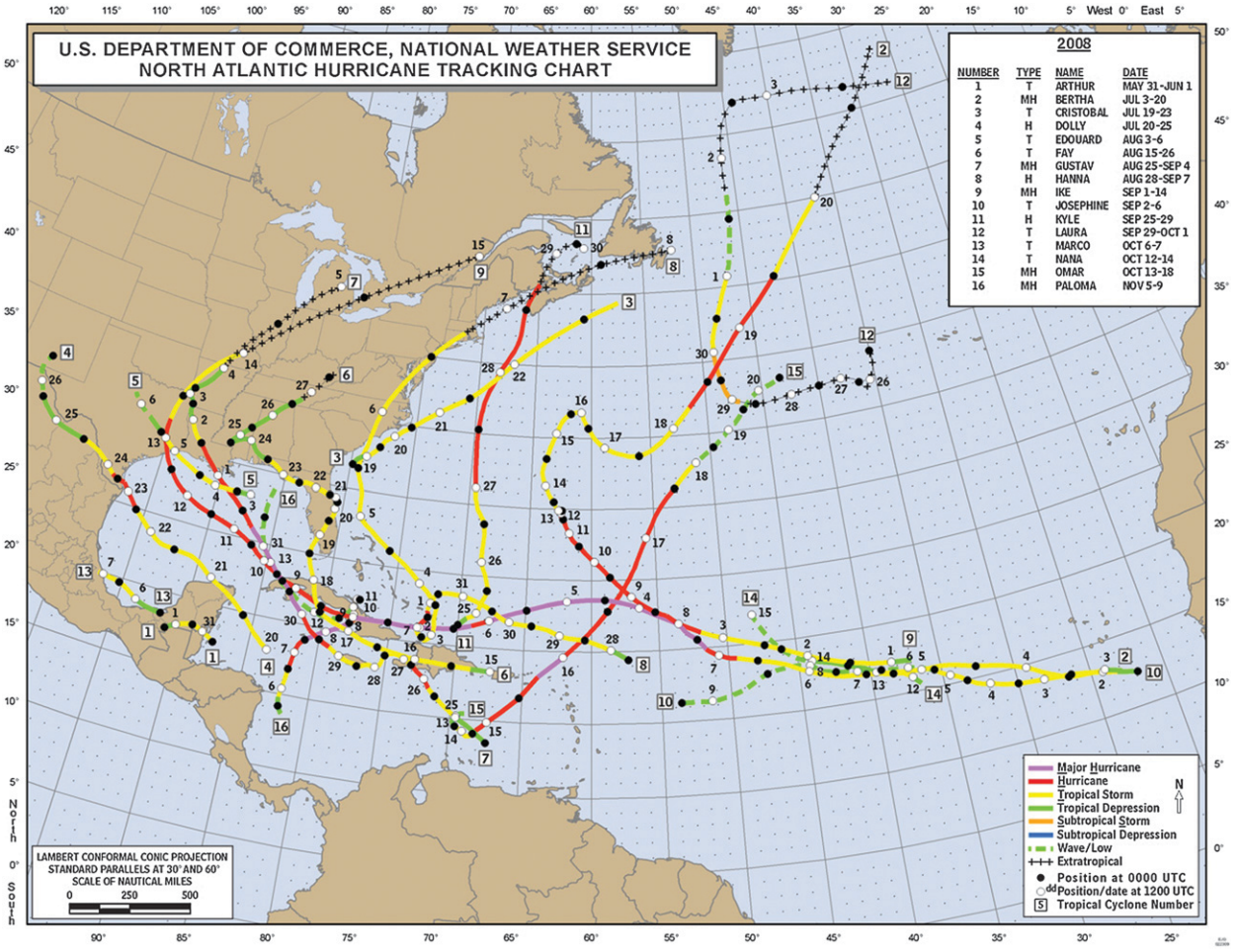

FIG. 1. Tracks of tropical storms and hurricanes in the Atlantic basin in 2008.

landfall in Cuba. Gustav and Ike both made landfall as category 4 hurricanes on the island within a 10-day period. Haiti was hit by Tropical Storm Fay and Hurricane Gustav and was adversely affected by heavy rains from Hurricanes Hanna and Ike, whose centers passed just north of Hispaniola. Hanna and Ike seriously impacted portions of the Turks and Caicos Islands. Omar was a major hurricane when it passed near the northern Leeward Islands and Paloma struck the Cayman Islands as a major hurricane.

Beginning with Dolly, six consecutive cyclones made landfall in the United States. Tropical Storm Edouard made landfall along the upper Texas coast in early August. Tropical Storm Fay produced record rainfalls in Florida as the center made four landfalls in the state. Dolly came ashore in southern Texas as a category 1 hurricane, while Ike made landfall near Galveston Island, Texas, as a very large category 2 hurricane.

The death toll from the Atlantic tropical cyclones is approximately 750. The majority of the deaths were the result of floods and mudslides in Haiti caused by heavy rains. Because four cyclones affected Haiti within a short period of time, it is not possible to separate the impacts of individual storms, and the death toll from each of the storms will likely never be known. In the United States, 41 deaths are directly attributed to the 2008 tropical cyclones, with nearly half of the deaths resulting from Hurricane Ike. Monetary damage from the season's tropical cyclones in the United States is estimated to be a little over $25 billion. Hurricanes Ike and Gustav produced most of the damage, about $19.3 and $4.3 billion, respectively. The $19.3 billion in damage from Ike makes it the fourth-costliest hurricane in U.S. history (Blake et al. 2007).

2. Storm and hurricane summaries

The individual cyclone summaries that follow are based on National Hurricane Center (NHC) poststorm meteorological analyses of a wide variety of (often

TABLE 1. 2008 Atlantic hurricane season statistics.

No.	Name	Class[a]	Dates[b]	Max 1-min wind (kt)	Min sea level pressure (mb)	Direct deaths	U.S. damage ($ million)[c]
1	Arthur	TS	31 May–1 Jun	40	1004	5	0
2	Bertha	MH	3–20 Jul	110	952	3	0
3	Cristobal	TS	19–23 Jul	55	998	0	0
4	Dolly	H	20–25 Jul	85	963	1	1050
5	Edouard	TS	3–6 Aug	55	996	1	Minor[d]
6	Fay	TS	15–26 Aug	60	986	13	560
7	Gustav	MH	25 Aug–4 Sep	135	941	112	4300
8	Hanna	H	28 Aug–7 Sep	75	977	500	160
9	Ike	MH	1–14 Sep	125	935	103	19 300
10	Josephine	TS	2–6 Sep	55	994	0	0
11	Kyle	H	25–29 Sep	75	984	0	0
12	Laura	TS	29 Sep–1 Oct	50	994	0	0
13	Marco	TS	6–7 Oct	55	998	0	0
14	Nana	TS	12–14 Oct	35	1004	0	0
15	Omar	MH	13–18 Oct	115	958	0	5
16	Paloma	MH	5–9 Nov	125	944	0	0

[a] Tropical storm (TS), wind speed 34–63 kt (17–32 m s^{-1}); hurricane (H), wind speed 64–95 kt (33–49 m s^{-1}); and major hurricane (MH), hurricane with wind speed 96 kt (50 m s^{-1}) or higher.
[b] Dates begin at 0000 UTC and include tropical and subtropical depression stages but excludes the remnant low and extratropical stages.
[c] Includes damage in U.S. territories (e.g., Puerto Rico and the U.S. Virgin Islands).
[d] Only minor damage was reported, but the extent of the damage was not quantified.

contradictory) data. Comprehensive descriptions of the data sources used by the National Hurricane Center to analyze tropical cyclones have been provided in previous seasonal summaries (e.g., Franklin and Brown 2008), and more recently by Rappaport et al. (2009).

These analyses result in the creation of a ''best track'' database for each cyclone, consisting of 6-hourly representative estimates of the cyclone's center position, maximum sustained (1-min average) surface (10-m) wind, minimum sea level pressure, and maximum extent of 34-, 50-, and 64-kt winds in each of four quadrants around the center. The best track identifies a system as a tropical cyclone at a particular time if NHC determines that it satisfies the following definition: ''A warm-core, nonfrontal synoptic scale cyclone, originating over tropical or subtropical waters with organized deep convection and a closed surface wind circulation about a well-defined center'' (Office of the Federal Coordinator for Meteorology 2008). The life cycle of each cyclone (Table 1) is defined to include the tropical or subtropical depression stage, but does not include remnant low or extratropical stages. The tracks and basic statistics for the season's tropical storms and hurricanes are given in Fig. 1 and Table 1, respectively. (Tabulations of the 6-hourly best-track positions and intensities can be found in the NHC tropical cyclone reports, available online at http://www.nhc.noaa.gov/pastall.shtml. These reports contain storm information omitted here because of space limitations, including additional surface observations and a forecast and warning critique.)

In the cyclone summaries below, U.S. property damage estimates have been generally estimated by doubling the insured losses reported by the Property Claim Services of the Insurance Services Office. The reader is cautioned, however, that great uncertainty exists in determining the cost of the damage caused by tropical cyclones. Descriptions of the type and scope of damage are taken from a variety of sources, including local government officials, media reports, and local National Weather Service (NWS) Weather Forecast Offices (WFOs) in the affected areas. Tornado counts are based on reports provided by the WFOs and/or the NWS Storm Prediction Center. The strength of a tornado is rated using the enhanced Fujita (EF) scale (Texas Tech University 2006). Tables of selected observations are also provided for many of the cyclones in an online supplement to this article. All dates and times are based on UTC time.

a. Tropical Storm Arthur, 31 May–1 June

The genesis of Arthur occurred when the lower- to midlevel remnants of eastern Pacific basin Tropical Storm Alma (Blake and Pasch 2010) interacted with a tropical wave over the northwestern Caribbean Sea. On 30 May, Alma's remnants moved across Honduras into the northwestern Caribbean Sea, which likely caused a large increase in convection near the wave axis and the development of a new surface low about 75 n mi southeast of Belize. Data from the National Aeronautics and Space Administration (NASA) Quick Scatterometer (QuikSCAT; Brennan et al. 2009) and ship observations

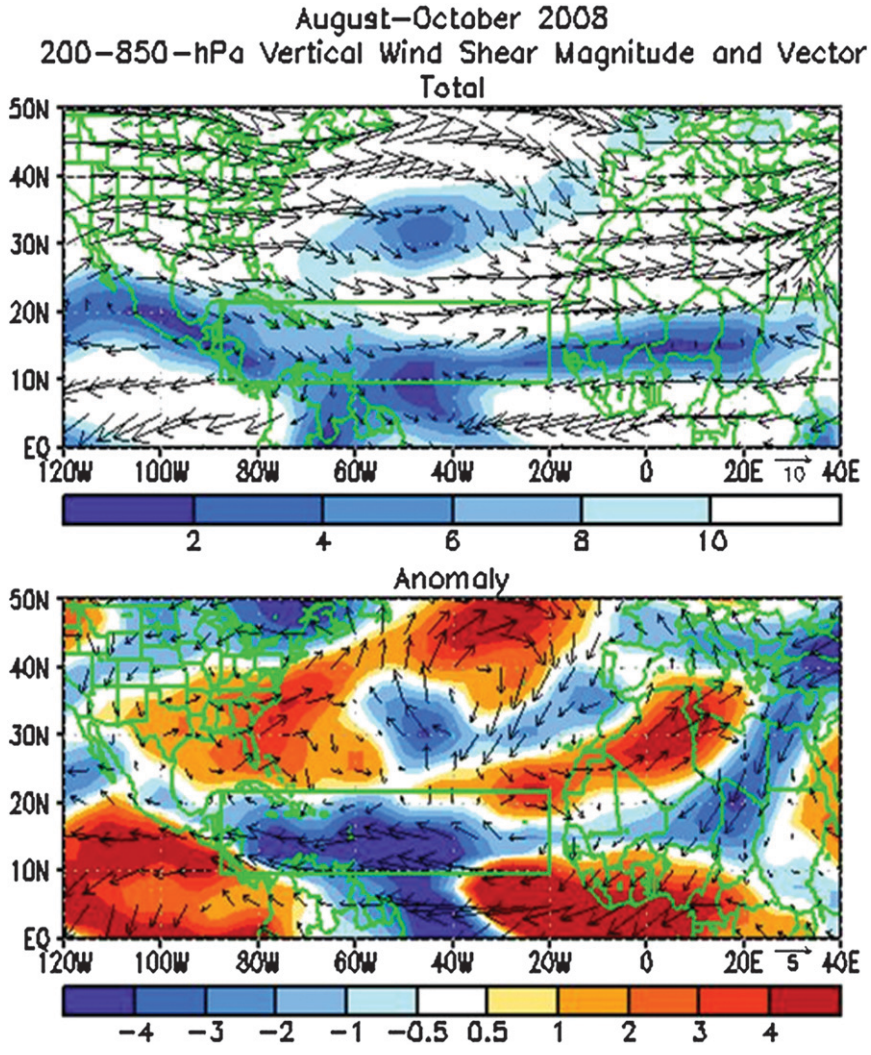

FIG. 2. August–October 2008 vertical wind shear (200–850 hPa) magnitude and (top) vectors and (bottom) anomalies in m s^{-1}. Anomalies are departures from the 1971–2000 base period monthly means. Images courtesy of the National Oceanic and Atmospheric Administration (NOAA)/Climate Prediction Center.

suggest that the low became sufficiently well defined to be considered a tropical storm around 0000 UTC 31 May, when it was centered about 45 n mi east of Belize City. Arthur moved slowly west-northwestward and reached a peak intensity of 40 kt 6 h later. The storm maintained this intensity through landfall, which occurred around 0900 UTC 31 May in northeastern Belize, about midway between Belize City and Chetumal, Mexico. Even after landfall, the cyclone continued to produce tropical storm–force winds in bands to the northeast of the center for almost 24 h. Arthur weakened to a tropical depression by 1200 UTC 1 June while centered about 15 n mi north of the northern border of Guatemala and Mexico. Twelve hours later, the system lost organized deep convection and degenerated into a broad area of low pressure. The remnants of the system continued moving slowly westward, producing areas of heavy rainfall over southern Mexico for the next couple of days.

Reports indicate that Arthur produced rainfall amounts of up to 375 mm in Belize. Five deaths were directly associated with Arthur, all due to flooding in Belize. The Belize National Emergency Management Organization estimated that the total damage caused by the storm was about $78 million [U.S. dollars (USD)].

b. Hurricane Bertha: 3–20 July

Bertha developed from a well-defined tropical wave that crossed the west coast of Africa on 1 July. The wave

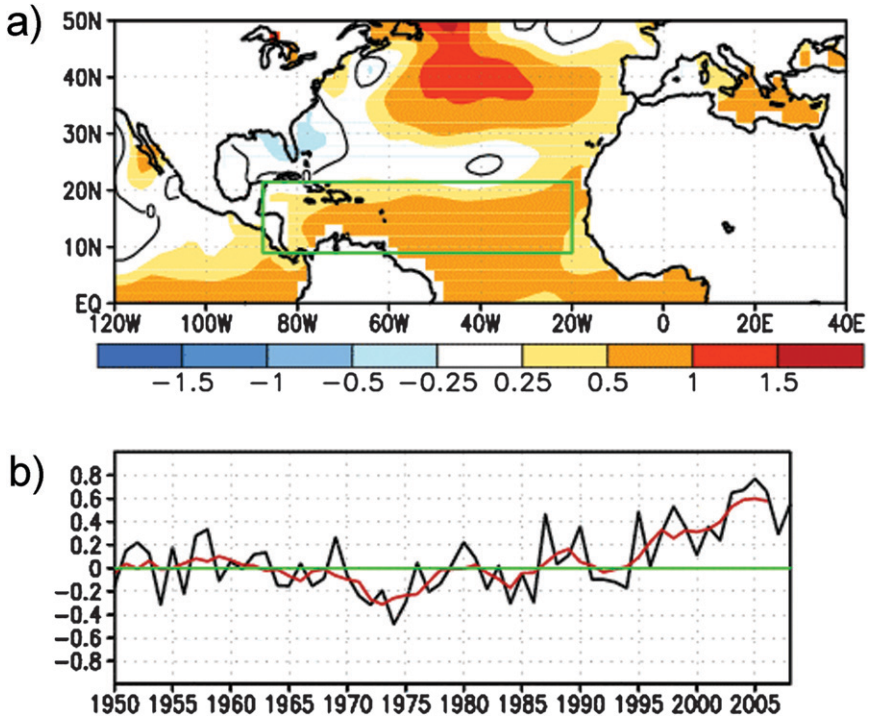

FIG. 3. (top) SST anomalies (°C) during August–October 2008. (bottom) Consecutive August–October area-averaged SST anomalies in the main development region (MDR). The red line shows the corresponding 5-yr running mean. The green box in (top) denotes the MDR. Anomalies are departures from the 1971–2000 period monthly means. Images courtesy of the NOAA/Climate Prediction Center.

was accompanied by a closed surface low and a large area of convection even before it emerged into the Atlantic. Within an environment of light vertical shear but marginally warm sea surface temperatures, the wave slowly developed, and by 0600 UTC 3 July had acquired enough organized convection to be designated a tropical depression about 220 n mi south-southeast of the Cape Verde Islands. The cyclone strengthened to a tropical storm 6 h later while passing south of the Cape Verde Islands. Bertha's strength changed little during the next couple of days as the storm moved quickly west-northwestward. The cyclone reached warmer waters by 6 July, and attained hurricane strength early on 7 July while centered about 750 n mi east of the northern Leeward Islands.

During the next several days, Bertha's intensity fluctuated because of varying atmospheric factors. On 7 July, as the cyclone turned northwestward, Bertha underwent a period of rapid intensification [30 kt or more intensity increase in 24 h; Kaplan and DeMaria (2003)], with its maximum sustained winds increasing by 45 kt during the 15-h period beginning at 0600 UTC that day. Advanced Dvorak Technique (ADT; Olander and Velden 2007) intensity estimates suggest that the hurricane reached a peak intensity of 110 kt at 2100 UTC 7 July. Bertha then encountered an environment of strong vertical shear on 8 July, resulting in a period of rapid weakening, but the cyclone reintensified on 9 July as the shear decreased.

On 10 July, an outer convective band began to wrap around the center, forming an outer eyewall. This resulted in some weakening of the hurricane. Some slight fluctuations in intensity were noted on 11 July. Bertha moved into an area of light steering currents on 12 July, which resulted in the cyclone becoming nearly stationary. Upwelling, induced by the cyclone while it was nearly stationary, likely caused the sea surface temperatures to decrease, and Bertha weakened to a tropical storm on 13 July. The next day, Bertha resumed its northward motion and brought tropical storm conditions to Bermuda while its center passed about 40 n mi to the east of the island (see supplemental Table S1).

The storm then turned eastward and southeastward on 16 July while it moved cyclonically around a large deep-layer low over the central Atlantic. Bertha accelerated northeastward the next day in the strong southwesterly flow ahead of a trough moving off the east coast of the United States, and became a hurricane again. Bertha passed about 400 n mi southeast of Cape Race, Newfoundland, on 19 July and became an extratropical

cyclone over the North Atlantic by 1200 UTC 20 July. The extratropical low continued northeastward toward Iceland, where it merged with a larger extratropical cyclone the next day. Bertha's 17.25 days as a tropical cyclone makes it the longest-lived Atlantic basin July tropical cyclone on record.

The highest winds reported on Bermuda were from two elevated observing sites: one at the Bermuda Maritime Operations Centre and the other on Commissioner's Point. The site at the Maritime Operations Centre reported sustained winds of 59 kt while the station at Commissioner's Point measured a wind gust to 79 kt (see supplemental Table S1).

Damage in Bermuda included broken tree branches and downed power lines that resulted in scattered power outages. Long-period swells generated by Bertha caused dangerous surf conditions and rip currents along much of the east coast of the United States. Over 1500 ocean rescues were reported in Ocean City, New Jersey, during a 7-day period beginning on 9 July, and 3 persons drowned along the New Jersey coast during the height of the event.

c. Tropical Storm Cristobal, 19–23 July

The development of Cristobal can be traced to the remnants of a frontal boundary that became nearly stationary along the east coast of the United States in mid-July. On 16 July, the decaying frontal trough extended southwestward across Florida and into the eastern Gulf of Mexico. An area of low pressure formed along the southern portion of the trough near the southwest coast of Florida that day. On 17 July, the low produced heavy rains over portions of the Florida Peninsula as it moved northeastward across the state, and shower activity associated with the system gradually increased and became more concentrated when the low was located near the coast of Georgia. Over the next day or so, the surface circulation gradually became better defined, resulting in the formation of a tropical depression by 0000 UTC 19 July, about 60 n mi east of the border between Georgia and South Carolina.

The newly formed depression moved slowly toward the northeast with most of the shower activity located to the east of the center. The surface circulation and convection continued to become better organized and the depression attained tropical storm strength by 1200 UTC 19 July. Cristobal maintained a northeastward motion and its center passed just southeast of the North Carolina Outer Banks early on 21 July. QuikSCAT data suggest that Cristobal reached a peak intensity of 55 kt around 0600 UTC 21 July. On 22 July, an eye feature was briefly observed in microwave imagery (not shown) when Cristobal was located about 180 n mi southeast of Cape Cod, Massachusetts. Shortly thereafter, Cristobal encountered cooler waters and began to weaken. The cyclone passed about 125 n mi southeast of the coast of Nova Scotia and was absorbed by a large extratropical cyclone by 1200 UTC 23 July.

While the center of Cristobal passed near the North Carolina coast, the strongest winds remained offshore and there was little impact on land. When Cristobal was still more than a day away from its closest approach to the Canadian Maritimes, rain moved out well ahead of the cyclone and became enhanced by a stalled frontal system over Nova Scotia. This resulted in intense rainfall, with the highest accumulations occurring along the coast of Nova Scotia.

d. Hurricane Dolly, 20–25 July

1) SYNOPTIC HISTORY

Dolly had its origins in a tropical wave that crossed the west coast of Africa early on 11 July. The system moved rapidly westward and generated a surface low pressure area about 1400 n mi east of the southern Windward Islands on 13 July. The low moved generally westward over the next several days, and while the associated deep convection appeared to be fairly well organized at times, there was little overall development. The system crossed the Windward Islands and entered the eastern Caribbean Sea early on 17 July. As the wave traversed the eastern and central Caribbean, observations from an Air Force Reserve Command (AFRC) Hurricane Hunter aircraft showed that the system had a broad low-level cyclonic flow but lacked a well-defined center of circulation. However, the wave was producing squalls with winds to tropical storm force during this period. On 20 July, when the system reached the western Caribbean Sea, the Hurricane Hunters found a well-defined circulation center, indicating the formation of a tropical cyclone at around 1200 UTC centered about 270 n mi east of Chetumal, Mexico. At the time of genesis, the system's maximum winds were already near 40 kt.

The storm moved northwestward and, for unknown reasons, soon became disorganized. Although the circulation center temporarily became difficult to track, surface data suggest that Dolly passed near the northeastern tip of the Yucatan Peninsula of Mexico around 0600 UTC 21 July. A little later that day, Dolly's circulation quickly became better defined just to the north of the Yucatan Peninsula. The steering flow associated with a midtropospheric high pressure area over the southeastern United States drove the storm west-northwestward, and then northwestward, toward the western coast of the Gulf of Mexico. An upper-level cyclone over the Bay of Campeche inhibited upper-tropospheric outflow over

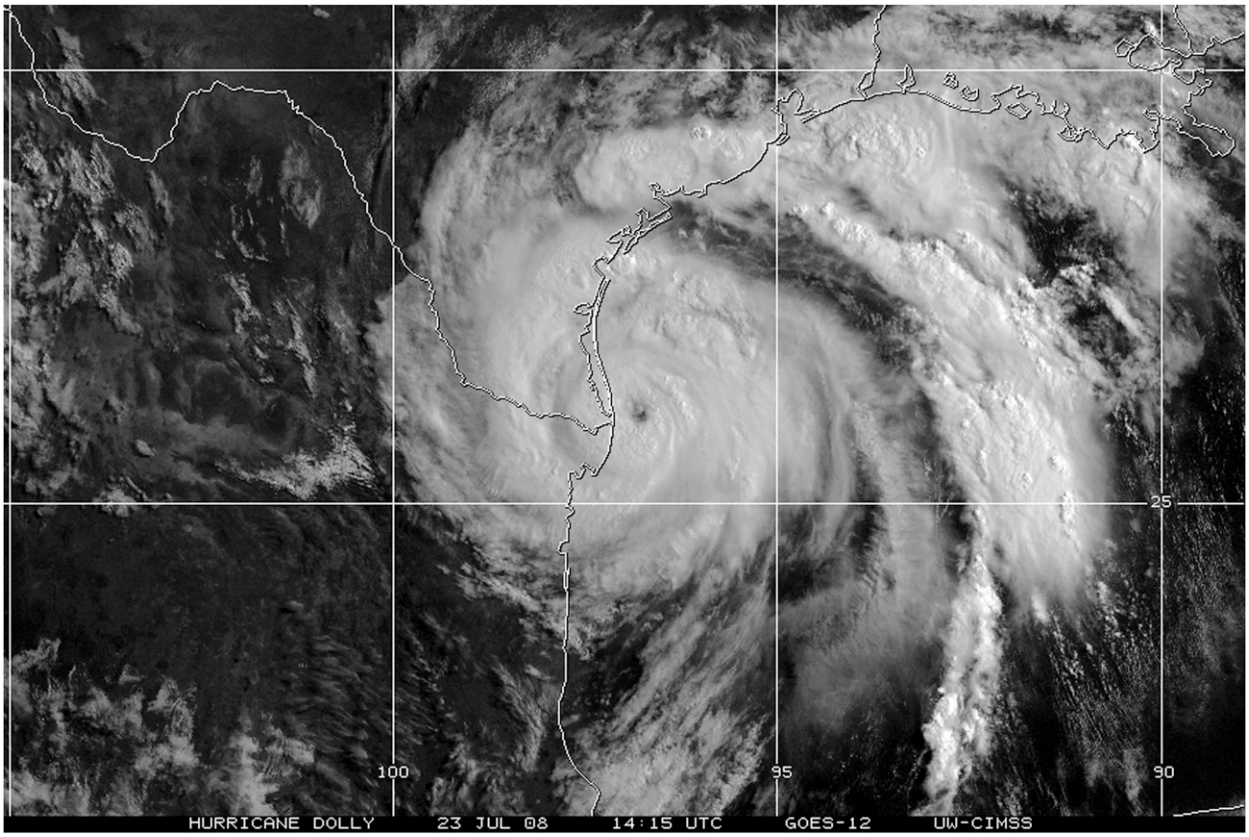

FIG. 4. Geostationary Operational Environmental Satellite-East (*GOES-12*) visible satellite image of Hurricane Dolly at 1415 UTC 23 Jul 2008, near the time of the cyclone's maximum intensity. Image courtesy of the University of Wisconsin—Madison.

the southern semicircle of Dolly on 21–22 July. By late on 22 July, however, the upper-level low moved farther away from the tropical cyclone and weakened, allowing an expansion of the outflow pattern, and Dolly strengthened into a hurricane by 0000 UTC 23 July. Meanwhile, a short-wave trough digging southward from the Great Lakes began to erode the midtropospheric ridge to the north of Dolly. The hurricane slowed its northwestward motion and strengthened as it approached the coast of extreme southern Texas and northeastern Mexico. Dolly reached its peak intensity of 85 kt, category 2 on the Saffir–Simpson hurricane scale, around 1400 UTC 23 July while it was centered a little less than 20 n mi east of the mouth of the Rio Grande (Fig. 4).

Over the ensuing 4 h prior to landfall, the hurricane weakened somewhat. Radar imagery showed that Dolly's eyewall, which was generally closed during the few hours before the time of maximum intensity, became open over the northern semicircle just prior to landfall. It is possible that the erosion of the eyewall was the result of drier air moving off of Mexico, wrapping around the southern part of the cyclone's circulation, and penetrating the northern part of the core of the hurricane. Another possible contributor to the weakening may have been the interaction of the slow-moving hurricane with cooler shelf waters along the coastline. Dolly made landfall at South Padre Island, Texas, just after 1800 UTC 23 July as a category 1 hurricane with estimated maximum winds of 75 kt. The center then made landfall on the Texas mainland 2 h later, about 10 n mi south of Port Mansfield, with an estimated intensity of 70 kt.

After landfall, Dolly weakened and became a tropical storm by 0600 UTC 24 July. Moving on a heading between northwest and west-northwest, the cyclone center crossed the Rio Grande around 1800 UTC 24 July, and Dolly weakened to a tropical depression over extreme northern Mexico by 0600 UTC 25 July. The system degenerated into a remnant low around 0000 UTC 26 July and then turned northward, crossing the Mexico–U.S. border near El Paso, Texas, around 1800 UTC 26 July. Although the surface low lost its identity over New Mexico early on 27 July, Dolly's upper-level remnant disturbance continued to produce locally heavy rainfall along its path over New Mexico for another day or so.

2) METEOROLOGICAL STATISTICS

The highest wind measured by a reconnaissance aircraft was 92 kt just after 1200 UTC 23 July at a flight level of 700 mb, corresponding to an intensity estimate of 83 kt using a 90% surface adjustment factor (Franklin et al. 2003). This measurement is the basis for the best-track maximum intensity estimate of 85 kt for Dolly. Near the time of Dolly's landfall in Texas, the maximum flight level wind was 85 kt, which corresponds to an intensity of 77 kt. Data from the NWS Weather Surveillance Radar-1988 Doppler (WSR-88D) from Brownsville, Texas, showed that the maximum Doppler velocity around the time of landfall in Texas was 93 kt at an elevation of 1900 ft. Using a 75% adjustment factor for that altitude yields an intensity estimate of 70 kt. Based on the aircraft-measured winds and the Doppler data, 75 kt is the estimate for Dolly's intensity at landfall in Texas. While the hurricane best-track database (HURDAT; Jarvinen et al. 1988) records Dolly as a category 1 landfall in Texas, it cannot be determined whether category 2 winds impacted the Texas coast during the few hours prior to landfall.

Selected surface observations from land stations and data buoys are provided in supplemental Table S2. A mast-mounted anemometer on a vehicle located at the coastline 21 n mi east of Matamoros, Mexico, measured a peak 1-min mean wind of 83 kt with a gust to 103 kt at an elevation of about 3 m AGL. These peak values occurred 4 h prior to landfall of the center in Texas near the time of Dolly's maximum intensity, when the observing site appeared to be near the radius of maximum winds. A Texas Tech University tower deployed on a sand dune on South Padre Island, Texas, measured a peak 1-min mean wind of 68 kt with a gust to 93 kt at an elevation of 2.25 m AGL.

Rainfall totals of 125–250 mm were recorded over portions of the lower Rio Grande Valley with a maximum total of 381 mm at Harlingen, Texas. These rains resulted in extensive inland flooding over the Rio Grande Valley region.

Storm surges of up to 1.22 m were observed at South Padre Island, Port Mansfield, and the Port of Brownsville, Texas. Water flowed eastward from the Laguna Madre, inundating the bay side of South Padre Island with around 1–1.25 m of water.

In Texas, two weak (EF0) tornadoes were reported in Cameron County. Two EF0 tornadoes were also observed in San Patricio County, and an EF0 tornado was also reported in Jim Wells County. A waterspout was sighted over Corpus Christi Bay.

3) CASUALTY AND DAMAGE STATISTICS

One death has been attributed to Dolly—a drowning in rough surf in the Florida Panhandle.

Total damage in the United States from Dolly is estimated to be $1.05 billion (USD). Dolly caused mainly moderate structural damage, primarily to roofs on South Padre Island. Damage in Brownsville was minor and consisted mainly of lost roofing material. Significant wind damage to trees and widespread power outages were reported across much of Cameron and Willacy counties in southern Texas.

e. Tropical Storm Edouard, 3–6 August

Edouard's origin can be traced to the remnants of a front that moved southward into the northern Gulf of Mexico on 2 August. Shower activity became more concentrated south of the Florida Panhandle along this weak surface trough during the day, and by early on 3 August a small area of low pressure had formed. By 1200 UTC that day the low had developed a well-defined circulation with sufficient convective organization to be designated a tropical depression; at this time the center was located about 140 n mi south of Pensacola, Florida.

The first aircraft mission into the depression, around 1930 UTC 3 August, found relatively light winds and a minimum pressure of 1007 mb on its first pass through the center. However, a burst of convection developed over the center about that time, and within an hour and a half the pressure had fallen to 1002 mb and flight-level winds had increased to 54 kt, indicating that the depression had strengthened to a tropical storm. This period of development was short lived, however, as northerly shear and midlevel dry air appeared to prevent the cyclone from maintaining convection over the center, and little change in strength occurred over the next 24 h as Edouard moved westward around the periphery of mid to upper-level high pressure over the south-central United States.

While the center of Edouard was passing around 50 n mi to the south of the coast of Louisiana late on 4 August, northerly shear abated. Turning to the west-northwest around the periphery of the mid- to upper-level high, Edouard began to strengthen. As it approached the upper Texas coast early on 5 August, spiral banding features became better defined. An 850-mb flight-level wind observation of 68 kt at 0704 UTC 5 August is the basis for Edouard's estimated peak intensity of 55 kt. Edouard maintained this intensity and made landfall at the McFaddin National Wildlife Refuge in Texas, between High Island and Sabine Pass, at 1200 UTC that day.

Edouard quickly weakened as it moved inland, becoming a depression near 0000 UTC 6 August and degenerating to a remnant low 6 h later when deep convection diminished. The remnant circulation of Edouard continued across central Texas, accompanied by intermittent convection, before dissipating later that day.

Along the northwestern coast of the Gulf of Mexico, sustained winds of 49 and 47 kt were observed at Texas Point, Texas, and Calcasieu Pass, Louisiana, respectively (see supplemental Table S3). The highest wind gust reported over land was 62 kt at Texas Point, near the Sabine Pass. Storm surge values did not exceed 1.2 m. The largest rainfall amounts occurred in a small area close to the path of the center; the highest observed storm total rainfall of 164.6 mm occurred at the Baytown, Texas, Emergency Operations Center. There were no tornadoes reported in association with Edouard.

Damage associated with Edouard was relatively light. In southwestern Louisiana, the roofs of several mobile homes were damaged and there were downed trees and power lines. Inland flooding closed a few roads, including a portion of Interstate 10 in Chambers County in Texas. Minor tidal flooding was reported in Lake Charles, Louisiana, and Gilchrist, Texas.

There was one death reported in association with Edouard—an adult male who fell overboard from a shrimping vessel in rough seas near the mouth of the Mississippi River.

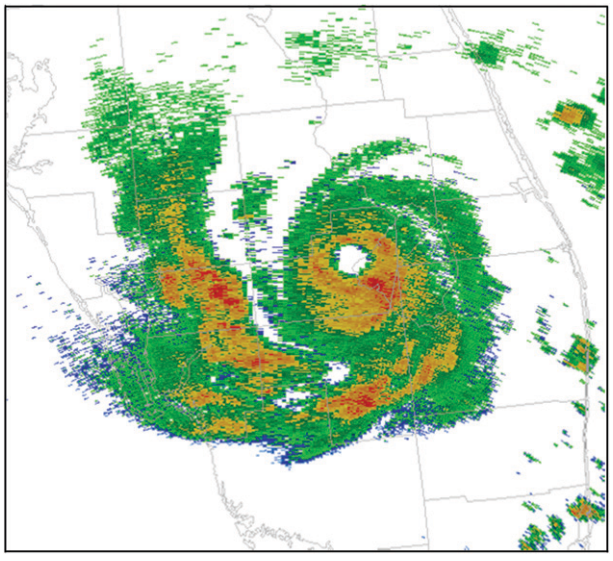

FIG. 5. WSR-88D radar reflectivity image of Tropical Storm Fay at 1811 UTC 19 Aug 2008, near the time of the cyclone's maximum intensity. At that time the center of Fay was located just northwest of Lake Okeechobee, Florida.

f. Tropical Storm Fay, 15–26 August

1) SYNOPTIC HISTORY

The tropical wave that spawned Fay emerged off the African coast on 6 August. The disturbance moved quickly west-northwestward across the tropical Atlantic Ocean, accompanied by limited thunderstorm activity. However, as the wave passed near the Leeward Islands on 14 August, its forward speed decreased and convective activity associated with the wave increased. Later that day, the system turned westward, and surface observations and QuikSCAT data indicated that a well-defined low pressure area had formed. However, the low moved westward along the southern coast of Puerto Rico, and development was inhibited because of the interaction of the circulation with the nearby terrain. By early on 15 August, the center of the low moved over the waters of the Mona Passage, and the convective organization of the system increased. Dvorak satellite classifications (Dvorak 1984) suggest that a tropical depression formed near 1200 UTC 15 August just west of the northwestern tip of Puerto Rico.

The depression moved westward around a strong subtropical ridge over the western Atlantic, and made landfall near El Cabo, Dominican Republic, at 1430 UTC 15 August. Flight-level wind data from reconnaissance aircraft indicate that the system became a tropical storm around 1800 UTC, even though the center of the cyclone was over land. Ship and aircraft data show that Fay remained a tropical storm as it traversed the southern portion of the Dominican Republic and Haiti. Before moving over the Windward Passage on 16 August, the center of Fay passed over Gonave Island, Haiti. The storm then turned west-northwestward and strengthened slightly, before making landfall along the south-central coast of Cuba about 20 n mi east of Cabo Cruz around 0900 UTC 17 August. Early on 18 August, Fay turned toward the northwest and made landfall again near Cienfuegos, Cuba, with maximum winds of 45 kt. After crossing Cuba, Fay emerged over the Straits of Florida around 1200 UTC that day and encountered moderate southwesterly vertical wind shear that inhibited significant strengthening. The cyclone made landfall near Key West, Florida, at 2030 UTC, with maximum winds still around 45 kt.

The vertical wind shear decreased after the center of Fay moved north of Key West, and data from land-based Doppler radars and reconnaissance aircraft indicated that the cyclone became better organized. The storm made landfall with 55-kt winds along the southwestern coast of Florida between Cape Romano and Everglades City at 0845 UTC 19 August. Shortly after landfall, an eye became apparent in both satellite and radar imagery (Fig. 5). Despite its center being over South Florida, Fay strengthened slightly and reached its peak intensity of 60 kt around 1800 UTC 19 August, when the center was near the western end of Lake Okeechobee. The eye remained apparent in radar imagery from 0929 UTC 19 August until 0212 UTC 20 August. Thereafter, Fay steadily weakened until the center reached the Atlantic

waters off the east-central Florida coast late on 20 August. Steering currents weakened the next day as a midlevel trough eroded the western portion of the subtropical ridge across Florida. This caused Fay to turn northward and slow to a forward speed of 3–4 kt, while the cyclone's center skirted the coastal region near Cape Canaveral. During this time, convective bands developed and persisted over east-central Florida. Because of the slow forward speed of Fay, these convective bands remained over the same areas for several hours, which led to widespread heavy rainfall in Brevard County, Florida.

As the midlevel trough lifted out to the north, a ridge began to build westward across the southeastern United States, and the tropical storm turned westward late on 21 August. Fay made its third Florida landfall near Flagler Beach around 1900 UTC 21 August. A general westward motion was maintained across the northern Florida peninsula and the cyclone emerged over the extreme northeastern Gulf of Mexico late on 22 August. Fay made its fourth Florida landfall—and eighth overall—just southwest of Carrabelle in the Florida Panhandle around 0615 UTC 23 August. The storm turned toward the westnorthwest shortly thereafter and weakened to a depression by 0000 UTC 24 August northeast of Pensacola, Florida. The depression moved slowly across extreme southern Alabama and Mississippi that day.

A midlevel trough moving southward and eastward from the central Plains caused the depression to begin moving northeastward on 25 August. During the next day or so, Fay moved across eastern Mississippi, northern Alabama, and extreme southeastern Tennessee before merging with a frontal boundary and becoming extratropical around 0600 UTC 27 August over eastern Tennessee. The extratropical low continued to move northeastward, and it was absorbed by a larger extratropical low over eastern Kentucky by 0600 UTC 28 August.

2) METEOROLOGICAL STATISTICS

The 60-kt peak intensity estimate for Fay at 1800 UTC 19 August is based on a combination of surface observations and NWS WSR-88D radar data from Melbourne, Miami, and Key West, Florida. Sustained winds of 54 kt were observed at an unofficial reporting station in Moore Haven, Florida, located south of the western end of Lake Okeechobee. Heavy rainfall was the most notable hazard caused by Fay. Fay's precursor disturbance produced heavy rainfall and localized flooding across Puerto Rico and the U.S. Virgin Islands. Fay also produced heavy rainfall in Hispaniola and Cuba. In the Dominican Republic, rainfall totals exceeding 250 mm occurred primarily over the southern half of the country. Numerous reporting stations in Cuba also received more than 250 mm of rainfall. Agabama, located in central Cuba, reported the greatest rainfall total in that country with 463 mm. In the United States, the heaviest rainfall occurred across Florida and southern Georgia. Rainfall maxima of 702.3 and 698.5 mm were measured near Melbourne, Florida, and Thomasville, Georgia, respectively (see supplemental Table S4). There were numerous rainfall reports of more than 500 mm across east-central Florida, and amounts in excess of 250 mm were common elsewhere across central and northern Florida, southwestern Georgia, and southeastern Alabama. Although significant floods occurred across east-central Florida, the runoff from that rainfall into the Kissimmee River Valley, as well as the rain that fell directly into Lake Okeechobee, helped to replenish the water level in the lake following extensive drought conditions that had prevailed for several months. Fay's traversal of southern and central Florida resulted in a beneficial 1.2-m rise in the water level of Lake Okeechobee.

Storm surge flooding from Fay was relatively minor. Most storm surge heights were generally 0.3–0.6 m along the South Florida coast, with up to 1.5 m reported in the Everglades City area. Higher surge values of 0.6–1.2 m were observed along the northeastern Florida coast, where Fay's slow forward speed during 20–22 August created a prolonged onshore southeasterly flow from the Atlantic Ocean.

In the United States, Fay produced a total of 81 tornadoes across five states: 19 in Florida, 17 in Georgia, 16 in North Carolina, 15 in Alabama, and 14 in South Carolina. Most of the tornadoes were categorized as EF0 intensity, although a few were classified at EF1 to EF2 intensity. An outbreak of 28 tornadoes occurred on 26 August across central and northern Georgia and western South Carolina.

3) CASUALTY AND DAMAGE STATISTICS

Fay was directly responsible for 13 deaths—5 in the Dominican Republic, 5 in Florida, and 3 in Haiti. There were also eight indirect deaths that mainly resulted from automobile accidents on wet roads. The deaths in the Dominican Republic occurred when vehicles were swept off roads by flood waters, and the deaths in Haiti occurred when a bus crossing the flood-swollen Riviere Glace was swept away.

Damage was primarily caused by rainfall-induced floods that affected mainly residential structures across the Dominican Republic, Haiti, and Florida. There were no reports of major damage or casualties in Cuba. The government of the Dominican Republic reported that more than 2400 homes were damaged or destroyed by wind or flood waters in that country. Media reports indicate that

extensive and devastating floods ravaged Haiti, especially on the island of Gonave. In Florida, the heavy rainfall resulted in more than 15 000 homes being flooded. Wind damage in the state was confined to mostly downed trees and power lines, plus minor roof damage to homes. An EF1 tornado that struck a manufactured housing community in Barefoot Bay, Florida, damaged 59 residences, 9 of which were declared uninhabitable. Total damage from Fay in the United States is estimated to be $560 million (USD).

g. Hurricane Gustav, 25 August–4 September

1) SYNOPTIC HISTORY

Gustav formed from a tropical wave that moved westward off the coast of Africa on 13 August. After briefly showing signs of organization on 18 August, westerly vertical wind shear prevented significant development during the next several days. The wave moved through the Windward Islands on 23 August, accompanied by a broad area of low pressure and disorganized shower activity. Late the next day, the organization of the convection associated with the system increased as it moved northwestward across the southeastern Caribbean Sea, and it is estimated that a tropical depression formed near 0000 UTC 25 August about 95 n mi northeast of Bonaire in the Netherlands Antilles.

The depression developed an unusually small inner wind maximum with a radius of about 10 n mi, and subsequently intensified rapidly. The cyclone became a tropical storm near 1200 UTC 25 August and a hurricane just after 0000 UTC 26 August. Gustav reached an intensity of 80 kt later on 26 August, and then weakened slightly before making landfall on the southwestern peninsula of Haiti near 1800 UTC that day. The center of Gustav crossed the peninsula into the Canal du Sud, and the cyclone weakened to a tropical storm by early 27 August.

A low- to midlevel ridge built over Florida and the western Atlantic Ocean on 27 August, and Gustav turned westward in response. Although the center was over water on 27 August, enough of the circulation was interacting with Hispaniola to cause Gustav's intensity to decrease to 40 kt late that day. Early on 28 August the storm moved southward, possibly due to a reformation of the center, and during this time Gustav's maximum winds increased to 60 kt. Little change in strength occurred before the center moved westward over Jamaica around 1800 UTC that day. The storm then turned west-northwestward early on 29 August and emerged off the western end of Jamaica about 1200 UTC. Later that day, Gustav entered an area of stronger southeasterly low- and midlevel flow on the southwestern side of the ridge.

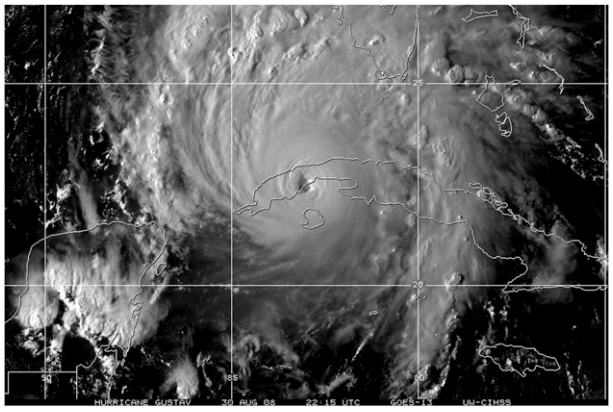

FIG. 6. *GOES-12* visible satellite image of Hurricane Gustav at 2215 UTC 30 Aug 2008, near the time of the cyclone's peak intensity and landfall just east of Palacios, Cuba. Image courtesy of the University of Wisconsin—Madison.

As a result, the cyclone began a northwestward motion at about 15 kt that would continue until its final landfall.

The cyclone intensified over the warm waters of the northwestern Caribbean Sea and regained hurricane status late on 29 August. Gustav became a category 2 hurricane as it moved through the Cayman Islands early on 30 August, and then attained category 4 strength before making landfall on the eastern coast of the Isle of Youth, Cuba, near 1800 UTC that day. A few hours later, as the hurricane made landfall in the Pinar del Rio province of western Cuba near 2200 UTC (Fig. 6), Gustav reached a peak intensity of 135 kt. The eye of Gustav emerged into the southeastern Gulf of Mexico early on 31 August.

Gustav weakened over Cuba, and it continued to weaken over the Gulf of Mexico on 31 August. An upper-level trough west of the hurricane caused some southerly vertical wind shear over the cyclone, and satellite imagery suggested that mid- to upper-level dry air became entrained into the circulation. These environmental factors appear to have prevented strengthening over the warm Gulf waters, although the hurricane grew substantially in size as it crossed the Gulf. By 1 September, tropical storm–force winds extended roughly 200 n mi from the center in the northeastern quadrant and hurricane-force winds extended roughly 70 n mi from the center in the same quadrant. Gustav made its final landfall near Cocodrie, Louisiana, around 1500 UTC 1 September with maximum winds near 90 kt (category 2).

The hurricane weakened to a tropical storm and its forward motion slowed as it crossed southern and western Louisiana later on 1 September. It became a tropical depression on 2 September over northwestern Louisiana. Gustav then meandered over southwestern Arkansas,

extreme northeastern Texas, and extreme southeastern Oklahoma on 3 September as it encountered weak steering currents at the western end of the Atlantic ridge. An approaching mid- to upper-level trough and accompanying cold front caused Gustav to accelerate northeastward on 4 September, and the cyclone became extratropical by 1200 UTC that day. The extratropical remnants of Gustav were absorbed by another extratropical low on 5 September as it moved through the Great Lakes region.

2) METEOROLOGICAL STATISTICS

The maximum 700-mb flight-level winds observed by reconnaissance aircraft in Gustav were 143 kt at 2014 UTC 30 August, with a 141-kt wind reported at 1654 UTC that day. The maximum surface wind estimated by the Stepped-Frequency Microwave Radiometer (SFMR; Uhlhorn et al. 2007) was 108 kt at 1658 UTC 30 August, and an eyewall dropsonde reported a surface wind of 108 kt 9 min earlier. The lowest central pressure reported by aircraft was 941 mb at 2154 UTC 30 August.

Selected surface observations from land stations and data buoys are given in supplemental Table S5. Gustav brought hurricane conditions to the southwest peninsula of Haiti, although no observations are available from this area. Gustav also produced hurricane conditions in portions of western Cuba, with the strongest winds reported at Paso Real de San Diego in Pinar del Rio province. Before being destroyed, this station (elevation 10 m) reported a 1-min wind of 135 kt at 2235 UTC 30 August with a peak gust of 184 kt, and is the basis for Gustav's estimated peak intensity. (The World Meteorological Organization has confirmed the observation as the highest wind gust in an Atlantic basin tropical cyclone.) Although the 135-kt observation is assumed to have been representative of the hurricane's intensity, radar data suggest the possibility that this observation may have been influenced by an eyewall mesovortex.

Hurricane conditions also occurred over portions of southern Louisiana. A National Ocean Service (NOS) station at the Southwest Pass of the Mississippi River (elevation 24 m) reported 6-min mean winds of 79 kt at 0918 UTC 1 September, with a gust to 102 kt. An offshore oil rig (elevation 122 m) reported sustained winds of 90 kt at 0505 UTC 1 September, with a gust to 108 kt. Strong winds accompanied Gustav well inland, with wind gusts of tropical storm force occurring as far north as central Arkansas.

Gustav likely caused a significant storm surge in western Cuba. No surge observations, however, are available from this area. The hurricane caused a widespread storm surge along the northern coast of the Gulf of Mexico, with above normal tides reported from the Florida Panhandle to the upper Texas coast, including Lake Pontchartrain (see supplemental Table S5). Surges of up to 4 m occurred along the Louisiana coast in the Mississippi Delta southeast of New Orleans, with surges of 2.7–3 m in other portions of southeastern Louisiana. The storm surge overtopped the levees and floodwalls in a few parts of the New Orleans metropolitan area. However, it did not cause widespread inundation of the city and its suburbs.

The highest rainfall amounts reported in Hispaniola from Gustav were 273.1 mm at Camp Perrin, Haiti, and 246.6 mm at Baharona, Dominican Republic. In Cuba, Central Rene Fraga and Perico in Matanzas province received 24-h totals of 271.8 and 271.5 mm, respectively. In Louisiana, a storm total of 533.4 mm of rain fell at Larto Lake.

Gustav is known to have produced 41 tornadoes: 21 in Mississippi, 11 in Louisiana, 6 in Florida, 2 in Arkansas, and 1 in Alabama. The strongest tornado was an EF2 in Evangeline Parish, Louisiana.

3) CASUALTY AND DAMAGE STATISTICS

Reports from relief agencies and the media indicate that Gustav was directly responsible for 112 deaths—77 in Haiti, 15 in Jamaica, 8 in the Dominican Republic, 7 in Louisiana, 4 in Florida, and 1 at sea. In addition, there were 41 deaths indirectly associated with Gustav in Louisiana. The deaths in the Dominican Republic were due to a landslide. Five deaths in Louisiana were due to falling trees, while the other two were caused by the EF2 tornado in Evangeline Parish. The deaths in Florida were drownings in rip currents that were caused by high surf produced by the hurricane.

Gustav caused considerable casualties and damage along its path. Significant property damage occurred in Haiti and the Dominican Republic, although monetary damage figures are not available. The storm caused $210 million (USD) in damage in Jamaica. Gustav's winds and tides caused major damage in western Cuba, particularly in the provinces of Pinar del Rio and the Isle of Youth. The government of Cuba estimated damage on the island to be about $2.1 billion (USD). In the United States, Gustav is estimated to have produced $4.3 billion (USD) in damage, with nearly half of that total occurring in Louisiana.

h. Hurricane Hanna, 28 August–7 September

Hanna formed from a tropical wave that entered the eastern Atlantic Ocean on 19 August. The wave spawned an area of low pressure on 26 August about 475 n mi east-northeast of the northern Leeward Islands. Additional

development of the system over the next day or two led to the formation of a tropical depression at 0000 UTC 28 August, about 275 n mi east-northeast of the northern Leeward Islands.

The overall organization of the system continued to increase, and it is estimated that the depression reached tropical storm strength 12 h later. Visible satellite imagery later that day, however, indicated that the center of Hanna was located near the western edge of the deep convection due to westerly shear from an upper-level low located northwest of the cyclone. Despite the moderate shear, the storm strengthened slightly as it moved in a general west-northwestward direction to the south of a subtropical ridge extending over the western Atlantic. The upper-level low shifted southward and gradually dissipated the next day, resulting in a low-shear environment conducive for strengthening. Deep convection began to form over the center of the storm around 0000 UTC 1 September. This development continued overnight and into the next morning, when a period of rapid intensification began. During that time, a deep-layer ridge building over the eastern United States caused Hanna to turn southwestward and to slow its forward speed. Reconnaissance aircraft data indicate that Hanna reached hurricane strength by 1800 UTC 1 September, while centered just north of the Caicos Islands.

A maximum 850-mb flight-level wind of 90 kt, observed late on 1 September, supports Hanna's estimated peak intensity of 75 kt near 0000 UTC 2 September, when the hurricane was centered over Providenciales in the Caicos Islands. Around that time a passive microwave image revealed the presence of a well-defined banded eye feature (not shown). However, no sooner had Hanna strengthened than it abruptly began to weaken, succumbing to the effects of moderate-to-strong northerly vertical wind shear associated with the building ridge over the United States, and Hanna weakened to a tropical storm by 1200 UTC 2 September.

During the time of Hanna's rapid weakening it moved on a general west-southwestward track, passing very near Great Inagua Island in the southeastern Bahamas. Hanna turned southeastward, with the center passing less than 30 n mi from the northern coast of Haiti early on 3 September. Later that day, Hanna interacted with another upper-level low over the Bahamas and exhibited a quasi-subtropical convective structure. The storm then turned northward and began to restrengthen as it moved over Middle Caicos Island shortly after 1800 UTC 3 September. Hanna completed a counterclockwise loop and began moving northwestward when a subtropical ridge built over the western Atlantic. During the next 24–36 h, Hanna's intensity remained between 55 and 60 kt while the center passed just east of the central and northwestern Bahamas. By 5 September, Hanna separated from the upper low and reached the western periphery of the subtropical ridge. The cyclone turned northward, its center passing about 150 n mi east of the coast of northern Florida. Hanna continued northward and accelerated, making landfall near the border of North and South Carolina at 0720 UTC 6 September with maximum winds of 60 kt. Once inland over North Carolina, the storm weakened while moving across the Mid-Atlantic region. Hanna turned northeastward and its center passed very close to New York City shortly after 0000 UTC 7 September. Shortly thereafter, the system became extratropical when it merged with a cold front over southern New England.

The extratropical remnant of Hanna moved over Nova Scotia during the afternoon of 7 September before turning east-northeastward, passing over southern Newfoundland early on 8 September. After moving offshore just east-northeast of St. John's, Newfoundland, the low-level circulation became ill defined as it merged with a second frontal boundary.

The 60-kt intensity estimate at the time of landfall in the United States is based on a peak 850-mb flight-level wind of 72 kt and an SFMR surface wind measurement of 58 kt. Selected surface observations from land stations and data buoys are given in supplemental Table S6. The highest sustained wind measured in the Caicos Islands was 54 kt at Pine Cay. Sustained tropical storm–force winds were reported at a few observing sites along the coast of the Carolinas and the Mid-Atlantic region of the United States. The highest sustained wind reported in the United States was 53 kt, with a gust of 63 kt, at the Johnny Mercer Pier at Wrightsville Beach, North Carolina.

Hanna produced very heavy rainfall over Hispaniola and Puerto Rico when its center passed just north and northwest of those islands. An observing site in Adjuntas, Puerto Rico, received 411.2 mm of rain. In Hispaniola, a maximum amount of 359.9 mm was reported at Oviedo, Dominican Republic, and 323.2 mm at Camp Perrin, Haiti. In the United States, Hanna produced a large swath of 75–125 mm of rain over the eastern United States. Some areas closer to Hanna's path received 125–180-mm totals, with a maximum amount of 245.1 mm at Woodbridge, Virginia. The extratropical remnant of Hanna produced 75–125 mm of rain over southern Maine, southern Newfoundland, and portions of Nova Scotia. The highest rainfall total observed in southeastern Canada was 145.3 mm at Saint John, New Brunswick. Hanna produced one EF1 tornado in the United States near Allentown, Pennsylvania.

In the southeastern Bahamas and the Turks and Caicos Islands some wind damage to roofs was reported.

Considerable flooding occurred in Five Cays and Providenciales. However, no casualties were reported in the Bahamas or Turks and Caicos Islands.

The heavy rainfall that occurred in Haiti was responsible for severe flooding and an estimated 500 fatalities. The heavy rains exacerbated the flooding situation caused by Tropical Storm Fay and Hurricane Gustav that passed near or over Haiti during the preceding three weeks. The hardest hit areas were in the northwestern portions of the country, particularly in the city of Gonaives. Because of the flooding from the previous storms and the subsequent impacts of Hurricane Ike the following week, it is difficult to determine the exact death toll in Haiti attributable to Hanna. Reports suggest that about 500 people died in Gonaives, most likely as a result of the flooding rains. Several hundred people remain missing and a final death toll from each of the storms will likely never be known.

In the mountainous regions of Puerto Rico, heavy rainfall produced a few mud slides that damaged some roads and bridges. Strong winds in some of the heavier squalls downed a few trees and power lines.

In the United States, Hanna produced an estimated $160 million (USD) in damage. Damage included downed trees and power lines, which resulted in numerous electrical disruptions. There were some reports of trees that fell on homes, but there were no injuries or deaths as a result. Storm surge flooding in southeastern North Carolina caused minor beach erosion and some flooding in low-lying areas along the Pamlico River. One indirect drowning death occurred in Georgetown County, South Carolina, when an automobile left the roadway and ended up in a flooded drainage ditch.

The remnants of Hanna were responsible for producing flooding and power outages in southeastern Canada.

i. Hurricane Ike, 1–14 September

1) SYNOPTIC HISTORY

Ike originated from a well-defined tropical wave that moved off the west coast of Africa on 28 August. An area of low pressure developed along the wave axis early the next day and produced intermittent bursts of convection as it passed south of the Cape Verde Islands during the next couple of days. The low gained sufficient convective organization to be designated as a tropical depression by 0600 UTC 1 September, about 675 n mi west of the Cape Verde Islands. The depression became a tropical storm 6 h later, but only slowly intensified over the next 2 days as it moved west-northwestward over the tropical Atlantic to the south of a strong subtropical ridge.

Visible and microwave satellite imagery indicated that strong convective banding had begun to wrap around the center of Ike by 1200 UTC 3 September. An eye became apparent by 1800 UTC, and Ike became a hurricane at that time when it was centered about 600 n mi east-northeast of the northern Leeward Islands. Around this time, a deep-layer low pressure area over the northwestern Atlantic weakened the subtropical ridge and allowed Ike to move on a west-northwestward track. Environmental conditions were favorable for strengthening and based on subjective and objective Dvorak satellite estimates, Ike is estimated to have strengthened from an intensity of 55 kt at 0600 UTC 3 September to its peak intensity of 125 kt (category 4) at 0600 UTC 4 September—a 70-kt increase over a 24-h period.

After Ike reached its peak intensity, an upper-level high located over the western Atlantic to the northwest of the hurricane began to strengthen. This resulted in strong northerly wind shear over the cyclone, causing the cloud pattern to become asymmetric. Weakening occurred over the next couple of days, and Ike briefly fell below major hurricane status at 1200 UTC 6 September. Microwave imagery at the time showed that much of the deep convection over the northern semicircle was severely eroded, including the northern eyewall, but a small eye remained.

Building midlevel high pressure over the western Atlantic caused the hurricane to turn to the west late on 4 September and the high became strong enough to induce an unclimatological west-southwesterly motion by 0000 UTC 6 September. While the hurricane was moving west-southwestward toward the Turks and Caicos Islands, northeasterly shear relaxed over the cyclone. Deep convection then redeveloped over the northern semicircle, and Ike regained category 4 status by 1800 UTC 6 September. Although the center of Ike passed just south of the islands around 0600 UTC 7 September, the northern eyewall passed directly over Grand Turk, Salt Cay, South Caicos, and a few other smaller cays. Ike then weakened to category 3 status, with maximum sustained winds of 110 kt, before making landfall on Great Inagua Island in the southeastern Bahamas around 1300 UTC 7 September.

Ike weakened a little more after passing over Great Inagua, but the hurricane regained category 4 status by 0000 UTC 8 September as it approached the coast of eastern Cuba (Fig. 7). Ike made landfall near Cabo Lucrecia around 0215 UTC with sustained winds estimated at 115 kt. The center traversed the provinces of Holguín, Las Tunas, and Camagüey during the early morning hours of 8 September, and Ike gradually lost strength, emerging over the waters of the northwestern Caribbean Sea around 1500 UTC with maximum

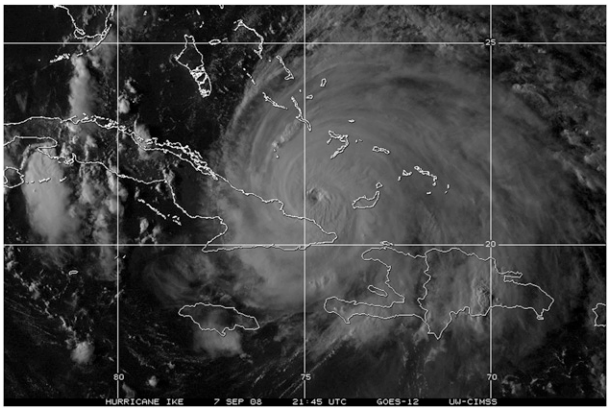

FIG. 7. *GOES-12* visible satellite image of Hurricane Ike at 2145 UTC 7 Sep 2008. Image courtesy of the University of Wisconsin—Madison.

sustained winds of 75 kt. Over the next day or so, Ike moved westward and maintained an intensity of 70 kt as its center moved along the southern coast of Cuba. Ike made a second landfall in western Cuba around 1400 UTC 9 September near Punta La Capitana, not far from the city of San Cristóbal, and then emerged over the Gulf of Mexico around 2030 UTC.

Ike's interaction with Cuba disrupted the hurricane's inner core and the wind field expanded as the hurricane moved into the Gulf of Mexico. The storm moved slowly northwestward on 10 September over the southeastern Gulf, and outer banding began to enclose the small eyewall that had survived the crossing of Cuba. This likely prevented rapid intensification and Ike's winds only strengthened to 85 kt by 1800 UTC 10 September. However, the extent of tropical storm and hurricane force winds increased, reaching as far as 240 n mi and 100 n mi from the center, respectively.

The subtropical ridge restrengthened by late on 10 September and caused Ike to turn back to the west-northwest over the central Gulf. The wind maximum associated with the outer banding began to contract and become the more dominant feature, and the inner wind maximum dissipated by 1800 UTC 11 September. Through the next day, Ike continued to lack inner-core convection while maintaining its large wind field, making it difficult for the system to intensify quickly.

Ike reached the western periphery of the subtropical ridge on 12 September and turned to the northwest toward the upper Texas coast. Microwave images and aircraft reconnaissance reports indicate that a 40 n mi diameter eye formed during the hours before landfall, and maximum winds increased to 95 kt. Ike turned to the north-northwest, and its center made landfall along the north end of Galveston Island, Texas, at 0700 UTC 13 September. The hurricane's center continued up through Galveston Bay, just east of Houston, then northward across eastern Texas. Ike weakened to a tropical storm by 1800 UTC 13 September just east of Palestine, Texas, and then became extratropical when it interacted with a front around 1200 UTC 14 September while moving northeastward through northern Arkansas and southern Missouri. The vigorous extratropical low moved quickly northeastward, producing hurricane-force wind gusts across portions of the Ohio Valley on the afternoon of 14 September. Thereafter, the low weakened and moved across southern Ontario and southern Québec and was absorbed by another cyclone near the St. Lawrence River by 1800 UTC 15 September.

2) METEOROLOGICAL STATISTICS

Ike's estimated peak intensity of 125 kt is based on the subjective Dvorak data T numbers and 3-h-averaged ADT estimates of 127 kt. Dvorak current intensity (CI) numbers supported maximum winds of 115 kt at the time of Ike's estimated peak intensity. The CI numbers, however, were constrained by Dvorak rules that limit the rate of intensification.

A Hurricane Hunter mission on the afternoon of 6 September, as Ike was approaching the Turks and Caicos Islands, measured a maximum flight-level wind of 129 kt and an SFMR estimate of 114 kt. These data support an intensity estimate of 115 kt. A reporting station on Grand Turk (78118) measured a sustained wind of 101 kt as the northern eyewall moved across the island (see supplemental Table S7).

The estimated landfall intensity in Cuba of 115 kt is based on an SFMR wind of 119 kt and a mean boundary layer wind of 131 kt reported by a dropwindsonde. The highest sustained winds reported in Cuba were 76 kt with a gust to 107 kt at Palo Seco, 77 kt with a gust to 104 kt at Puerto Padre, and 70 kt with a gust to 100 kt at Velasco (see supplemental Table S7).

Ike's minimum pressure over the Gulf of Mexico, as determined by a dropwindsonde, was 944 mb near 0000 UTC 11 September. The unusually broad distribution of strong winds associated with Ike when it was over the Gulf of Mexico resulted in minimum central pressures that were much lower than would be expected, given Ike's intensity.

The estimated Texas landfall intensity of 95 kt is based on flight-level winds of 105 kt, SFMR winds of up to 90 kt, and Doppler velocities from the NWS WSR-88D in Houston, which showed 114-kt winds at 6500 ft. The highest 1-min sustained wind recorded by surface instruments was 83 kt from a WeatherFlow anemometer located at Crab Lake, Texas, on the Bolivar Peninsula. The same instrument also reported a maximum 3-s

gust of 97 kt. A 1-min mean wind of 71 kt was recorded by a Texas Tech University Hurricane Research Team (TTUHRT) anemometer near Winnie, Texas, between Houston and Beaumont. A 3-s gust of 95 kt was reported by a separate TTUHRT sensor near Hankamer, Texas.

The extratropical remnants of Ike produced strong wind gusts as it moved across the Ohio Valley into southeastern Canada. The strongest gusts were 65 kt at both Louisville, Kentucky, and Columbus, Ohio. Hurricane-force wind gusts were also reported at Cincinnati and Wilmington, Ohio.

While storm surge associated with Ike affected the Turks and Caicos Islands, the southern Bahamas, and Cuba, there were no available measurements of water level heights from these areas. Unofficial and state television reports from Cuba indicated that storm surge and large waves as high as 50 ft washed over and damaged coastal homes and other structures in the city of Baracoa near Ike's first landfall in Cuba.

Higher-than-normal water levels affected virtually the entire U.S. Gulf Coast. As the hurricane grew in size, its large wind field pushed water toward the coastline well before Ike's center made landfall near Galveston, Texas. The highest storm surge measured by any NOS tide gauge was at Sabine Pass North, Texas, where 3.90 m was recorded at 0748 UTC 13 September, just as Ike was making landfall at Galveston. Port Arthur, located several miles inland at the head of Sabine Lake, measured a maximum surge of 3.36 m.

The highest storm surge occurred on the Bolivar Peninsula and in parts of Chambers County, Texas (including the east side of Galveston Bay), roughly from the Galveston Bay entrance to just northeast of High Island. While complete tide gauge records for this area are unavailable since many of the sensors failed from saltwater intrusion and large wave action, ground assessment teams determined that the surge was generally between 4.5 and 6.1 m. The highest water mark, collected by the Federal Emergency Management Agency was 5.33 m (relative to North American Vertical Datum of 1988) located about 10 n mi inland in Chambers County. Water depths of at least 1.22 m covered all of the Bolivar Peninsula, with most areas covered by at least 3 m of water (not including wave action). Much of the southern part of Chambers County was also inundated by at least 3 m of water.

Storm surge levels on Galveston Island and on the west side of Galveston Bay are estimated to have been between 3 and 4.5 m. Here, too, several NOS tide gauges failed, although the gauge at Eagle Point on the west side of Galveston Bay recorded a maximum surge of 3.50 m. The highest inundation in this area, at least 3 m, occurred on the bay side of Galveston Island, along the coast of mainland Galveston County, as well as over Apffel Park at the northern tip of Galveston Island.

NOS tide gauges indicated that water levels along the Texas and southwest Louisiana coasts began to rise rapidly on 12 September, approximately 24 h before the time of landfall. Numerous media reports the day before landfall showed water had already flooded areas near the coast and cutoff evacuation routes from areas such as the Bolivar Peninsula, well before strong winds reached the coast. By the evening of 12 September, about 6–8 h before landfall, storm tides were already running near 2.5 m in the vicinity of Galveston.

Although rainfall observations from the Turks and Caicos Islands and the southern Bahamas were scarce, reports from the Morton Salt Company indicated that 127–178 mm of rain fell on Great Inagua. Comprehensive rainfall totals from Haiti were also unavailable, but heavy rains there caused more flooding and mud slides in areas that were still recovering from Tropical Storm Fay and Hurricanes Gustav and Hanna. In Cuba, the highest reports were 349.8 mm at Júcaro and 307.6 mm at Topes de Collantes.

In the United States, Ike's outer rainbands produced some heavy rainfall over southern Florida. The highest reports were 160.8 mm near Ochopee and 151.9 mm near Chokoloskee. Ike produced a large area of rainfall 75 mm or greater over much of southeastern Texas and extreme southwestern Louisiana. The highest amount reported was 480.1 mm just north of Houston. The remnants of Ike produced heavy rainfall and exacerbated flooding across portions of Missouri, Illinois, and Indiana; the rainfall event over the Midwest was initiated a day before the cyclone's passage as remnant moisture from eastern North Pacific Tropical Storm Lowell (Blake and Pasch 2010) combined with a frontal system.

Twenty-nine tornadoes were reported in association with Ike in the United States. Two tornadoes occurred in the Upper Florida Keys when the outer spiral bands moved across the area. During 12–14 September, 17 tornadoes occurred in Louisiana, 1 in Texas, and 9 in Arkansas. None of these were rated higher than EF1.

3) Casualty and damage statistics

Ike was directly responsible for 103 deaths across Hispaniola, Cuba, and parts of the U.S. Gulf coast. Extensive damage from strong winds, storm surge, and rainfall occurred over Hispaniola, the Turks and Caicos Islands, the southern Bahamas, Cuba, and the U.S. Gulf of Mexico coast from Florida to Texas. Additional deaths and significant damage occurred across parts of the Ohio Valley and southeastern Canada after Ike lost tropical characteristics.

In Haiti, 74 deaths were directly attributable to Ike. Two deaths were reported in the Dominican Republic.

The Caribbean Disaster Emergency Response Agency estimated that 95% of the houses on Grand Turk and South Caicos were damaged, with nearly a third of the homes sustaining significant damage or complete destruction. Approximately 70%–80% of the houses on Great Inagua Island sustained roof damage, and 25% had major damage or were destroyed. Risk Management Solutions estimated that total damage costs were between $50 and $200 million (USD) for Turks and Caicos and the Bahamas.

Ike damaged 323 800 homes in Cuba, of which about 43 000 were a total loss, mainly in the provinces of Holguín, Las Tunas, Camagüey, Villa Clara, Santiago de Cuba, Guantanamo, Pinar del Rio, and the Isle of Youth. Seven direct deaths were reported in Cuba and the Cuban government estimated damage on the island to be around $7.3 billion (USD).

Official counts and media reports indicate that 20 people died in Texas, Louisiana, and Arkansas as a direct result of Ike. Twelve fatalities were reported in Galveston and Chambers Counties, Texas, where the worst storm surge occurred, and several bodies were found within debris fields on the bay side of the Bolivar Peninsula, on Goat Island, and on the north side of Galveston Bay in Chambers County. Three other drowning deaths were reported across Texas—one person drowned in the waters off Corpus Christi, one from storm surge in Orange County near Beaumont, and one after falling off a boat on Lake Livingston in Trinity County. In addition, one death in Montgomery County and one in Walker County resulted from trees falling onto the roofs of occupied houses. Reports from the Laura Recovery Center indicate that 25 people remained missing as of 17 September 2009. Two people died in Louisiana and one death occurred in Arkansas, when a tree fell on a mobile home. In addition to the direct deaths, as many as 64 indirect deaths were reported in Texas due to factors such as electrocution, carbon monoxide poisoning, and preexisting medical complications.

Significant storm surge and wave action along the upper Texas coast devastated the Bolivar Peninsula and parts of Galveston Island. Almost every structure on parts of the Bolivar Peninsula, including the communities of Crystal Beach, Gilchrist, and High Island, were completely razed from their foundations. Protected by a seawall, much of the city of Galveston was spared direct impact by storm surge and wave action from the Gulf of Mexico; however, the city was still inundated by surge when water rose on the north side of the island from Galveston Bay. Ike downed numerous trees and power lines across the Houston area, and many streets were blocked because of floodwaters. An estimated 2.6 million customers lost electrical power in Texas and Louisiana. Downtown Houston was spared significant wind damage, but streets were littered with traffic signals and glass. In southwestern Louisiana, storm surge waters pushed up to 30 miles inland, reaching areas near Lake Charles, and inundated homes in parts of Cameron, lower Vermilion, St. Mary, and Terrebonne Parishes.

The U.S. Department of Energy reported that 14 oil refineries were closed by the storm, as well as two Texas strategic petroleum reserve sites, causing rising gas prices and gas shortages across parts of the United States. In addition, the storm destroyed at least 10 offshore oil rigs and damaged several large pipelines.

The total damage in the United States from Ike is estimated to be $19.3 billion (USD). This ranks Ike as the fourth costliest hurricane to affect the United States, after Hurricanes Katrina (2005), Andrew (1992), and Wilma (2005).

The extratropical remnants of Ike caused several deaths and produced significant wind damage across the Ohio Valley. At least 28 direct and indirect deaths were reported in Tennessee, Ohio, Indiana, Illinois, Missouri, Kentucky, Michigan, and Pennsylvania. In Ohio, almost 2.6 million people lost power with the most extensive damage reported in the areas near Cincinnati, Columbus, and Dayton. The extratropical remnants produced an estimated $2.3 billion (USD) in nonflooding related insured losses. Insured losses in Ohio are estimated at $1.1 billion (USD), rivaling the 1974 Xenia tornado as the costliest natural disaster in that state's history.

In Canada, high winds and record rainfall were reported across portions of southern Ontario and Québec from the remnants of Ike.

j. Tropical Storm Josephine, 2–6 September

A strong tropical wave with an associated surface low departed the west coast of Africa late on 31 August. Convection associated with the low began to increase in organization on 1 September. By 0000 UTC 2 September, when the system was about 275 n mi south-southeast of Sal in the Cape Verde Islands, it had enough convective organization to be classified as a tropical depression. The cyclone is estimated to have become a tropical storm 6 h later, when a strong burst of convection formed near the center.

Josephine moved generally westward to west-northwestward at about 10 kt to the south of a midtropospheric ridge. The cyclone continued to strengthen on 2 September, reaching a peak intensity of 55 kt on 3 September. However, an upper-level trough between Josephine and Hurricane Ike caused vertical wind shear

to increase late on 3 September, and Josephine began to weaken. Deep convection associated with Josephine became less organized during the next couple of days as the tropical cyclone encountered slightly cooler waters and more stable air, while the shear remained strong. The system briefly moved northwestward on 5 September and slowed its forward motion. After a flare-up of convection overnight, thunderstorms diminished during the day, and Josephine weakened to a tropical depression early on 6 September, about 725 n mi west of Sal. Six hours later, devoid of deep convection, the system degenerated into a remnant low. The low moved westward for a couple of days, sped up, and turned southwestward on 9 September. The low dissipated early on 10 September, about 450 n mi east of Guadeloupe.

k. Hurricane Kyle, 25–29 September

The development of Kyle was associated with a tropical wave that moved off the coast of Africa on 12 September. The wave and an associated low pressure area crossed the Windward Islands on 19 September. The low turned toward the northwest and became separated from the wave, which continued moving westward across the Caribbean Sea. The low was centered near Puerto Rico on 21 September, and continued drifting northwestward and crossed Hispaniola over the next couple of days while producing disorganized thunderstorms. During this period, aircraft reconnaissance and surface data indicated that the system lacked a well-defined circulation center.

As the low moved northeastward away from Hispaniola, it finally developed a well-defined surface circulation center and it is estimated that a tropical depression formed at 0000 UTC 25 September about 100 n mi north of the Dominican Republic. Shortly thereafter, westerly wind shear that initially kept the center to the west of the convection relaxed, and convective bands began to wrap around the center. The improved convective organization, as well as a ship observation of 40 kt, indicates that the depression attained tropical storm strength around 0600 UTC. Kyle then moved on a northward track and gradually intensified, becoming a hurricane at 1200 UTC 27 September about 300 n mi west of Bermuda. Kyle continued moving between the north and north-northeast, and data from a dropsonde released by reconnaissance aircraft suggest the hurricane reached a peak intensity of 75 kt at 1200 UTC 28 September. Thereafter, as the convection started to become elongated and asymmetric, the cyclone began to lose tropical characteristics, but it made landfall as a 65-kt hurricane on the western tip of Nova Scotia just north of Yarmouth at 0000 UTC 29 September. Kyle continued rapidly northward and northeastward, developed a frontal structure and became extratropical. It was absorbed by a large extratropical low at 1800 UTC 30 September.

Kyle's precursor low produced torrential rains (up to 762 mm) and numerous flash floods and mud slides in Puerto Rico resulting in 6 deaths. Winds from Kyle (see supplemental Table S8) caused minor damage in Nova Scotia. Storm surge and waves produced minor street flooding in Shelburne, Nova Scotia.

l. Tropical Storm Laura, 29 September–1 October

Laura originated from an extratropical cyclone that formed along a quasi-stationary front a few hundred miles west of the Azores on 26 September. During the ensuing day or so, the cyclone intensified, due to baroclinic energy sources, and acquired hurricane-force winds on 27 September. Over the next couple of days the cyclone moved westward while the associated frontal features gradually dissipated, and unorganized deep convection developed within the system's circulation. The cyclone's maximum winds had decreased to near 50 kt by 28 September. Early the next day, a prominent band of deep convection formed over the southeastern semicircle of the cyclone; however, the convection was not concentrated near or over the center, and the system was collocated with an upper-tropospheric low pressure area. Therefore, it is estimated that the system transformed into a subtropical storm near 0600 UTC 29 September, centered about 650 n mi south-southeast of Cape Race, Newfoundland.

Laura turned from a west-northwestward to a north-northwestward heading as it moved between an area of high pressure to the north of the Azores and an extratropical low over the Canadian Maritimes. By early on 30 September Laura was moving northward while maintaining an intensity of near 50 kt. Although the system had acquired some warm-core structure, it had minimal deep convection and was still too coincident with the upper-tropospheric low to be considered a tropical cyclone. A little later on 30 September, the upper-level low became separated from the center of Laura, the radius of maximum winds contracted to near 60 n mi, and moderately deep convection became more organized and concentrated near the center of circulation. Based on these changes, it is estimated that the system became a tropical storm around 1200 UTC 30 September. Maximum winds remained near 50 kt as Laura traversed sea surface temperatures of around 26°C. By early on 1 October, the cyclone began to gradually weaken as it moved over cooler waters. Laura's peak winds decreased to 40 kt by 1200 UTC 1 October, and its deep convection diminished to the point that it could no longer be designated a tropical cyclone. There was little

evidence of frontal structure within the system at that time, indicating that Laura had become a remnant low. The low accelerated northward and surface analyses suggest that the system became embedded within a front by 0600 UTC 2 October, marking its transformation into an extratropical cyclone. Around 0600 UTC 3 October, the cyclone turned eastward and slowed its forward motion while becoming a hurricane-force extratropical cyclone for a second time. The system then accelerated eastward while gradually weakening and finally became absorbed within a larger extratropical cyclone several hundred nautical miles west of the British Isles on 4 October.

m. Tropical Storm Marco, 6–7 October

Marco formed out of a broad area of low pressure that had persisted over the northwestern Caribbean Sea and Yucatan Peninsula for several days at the end of September. By 4 October, when a tropical wave reached the western Caribbean Sea, a small circulation center became better defined near Belize. The area of low pressure then moved inland over the Yucatan Peninsula, temporarily hindering development. As the low approached the Bay of Campeche, however, convection increased and it is estimated that a tropical depression formed around 0000 UTC 6 October, when the system was centered over the Terminos Lagoon in the state of Campeche, Mexico.

The depression moved westward and entered the Bay of Campeche proper several hours later. The cyclone, whose convective cloud shield measured no more than about 75 n mi across, quickly developed banding features and strengthened, becoming a tropical storm by 1200 UTC about 60 n mi northeast of Coatzacoalcos. With a favorable anticyclonic flow aloft, Marco continued to strengthen as it moved west-northwestward over the Bay of Campeche. Reconnaissance aircraft dispatched to the cyclone on the afternoon of 6 October revealed a potent but tiny circulation. The aircraft measured a peak 925-mb flight-level wind of 61 kt about 5 n mi from the center at 2021 UTC, with a peak SFMR observation of 53 kt. These data suggest that Marco reached an intensity of about 55 kt by 0000 UTC 7 October, when it was centered about 65 n mi east-northeast of Veracruz. Marco then turned west with little apparent change in strength, making landfall east of Misantla, between Tuxpan and Veracruz, at 1200 UTC that day. The tiny circulation quickly weakened after landfall and dissipated shortly after 1800 UTC.

Data from the reconnaissance flight indicated that the radial extent of tropical storm–force winds was no more than 15 n mi, and high-resolution QuikSCAT data from a few hours later (0052 UTC 7 October) suggested that the tropical storm–force wind radii at that time were no larger than 10 n mi. The National Hurricane Center began including storm size (the maximum radial extent of 64-, 50-, and 34-kt winds in each of 4 quadrants surrounding the cyclone) in its best-track database beginning in 2004. A digital record of comparable operational estimates for the Atlantic basin is available beginning in 1988. Using the largest nonzero 34-kt wind radius as a metric for size, Marco's 10 n mi radial extent of tropical storm–force winds makes it the smallest tropical storm in this admittedly short record. Figure 8 shows the distribution of instantaneous rainfall rate based on satellite radar imagery near the time of Marco's maximum intensity. The figure shows both the convective structure and the extremely small size of the cyclone.

The impacts in Mexico from Marco were relatively minor.

n. Tropical Storm Nana, 12–14 October

Nana originated from a tropical wave that moved across the west coast of Africa coast on 6 October. QuikSCAT data indicate that the wave was accompanied by a broad cyclonic circulation. Convection associated with the wave was initially minimal, but gradually increased over the next few days. Around 0600 UTC 12 October, the convective activity became organized enough to designate the system as a tropical depression when it was centered about 690 n mi west of the Cape Verde Islands.

The depression moved west-northwestward toward a weakness in the subtropical ridge and strengthened into a tropical storm 6 h later. Surface wind estimates from the Advanced Scatterometer (ASCAT) and QuikSCAT between 1200 UTC 12 October and 0000 UTC 13 October indicate that Nana's peak winds were around 35 kt. During that time, Nana moved into a region of moderate-to-strong upper-level westerly winds that initiated weakening. Nana became a tropical depression at 1200 UTC 13 October, when it was centered about 870 n mi west of the Cape Verde Islands. The strong westerly wind shear continued to displace the convection well to the east of the center, and Nana degenerated into a nonconvective remnant low on 14 October. The remnant low turned northwestward ahead of a strong frontal system and dissipated around 1200 UTC 15 October about 820 n mi east-northeast of the Leeward Islands.

o. Hurricane Omar, 13–18 October

1) SYNOPTIC HISTORY

Omar originated from an easterly wave that moved westward from the coast of West Africa on 30 September. The wave reached the Lesser Antilles on 9 October, and

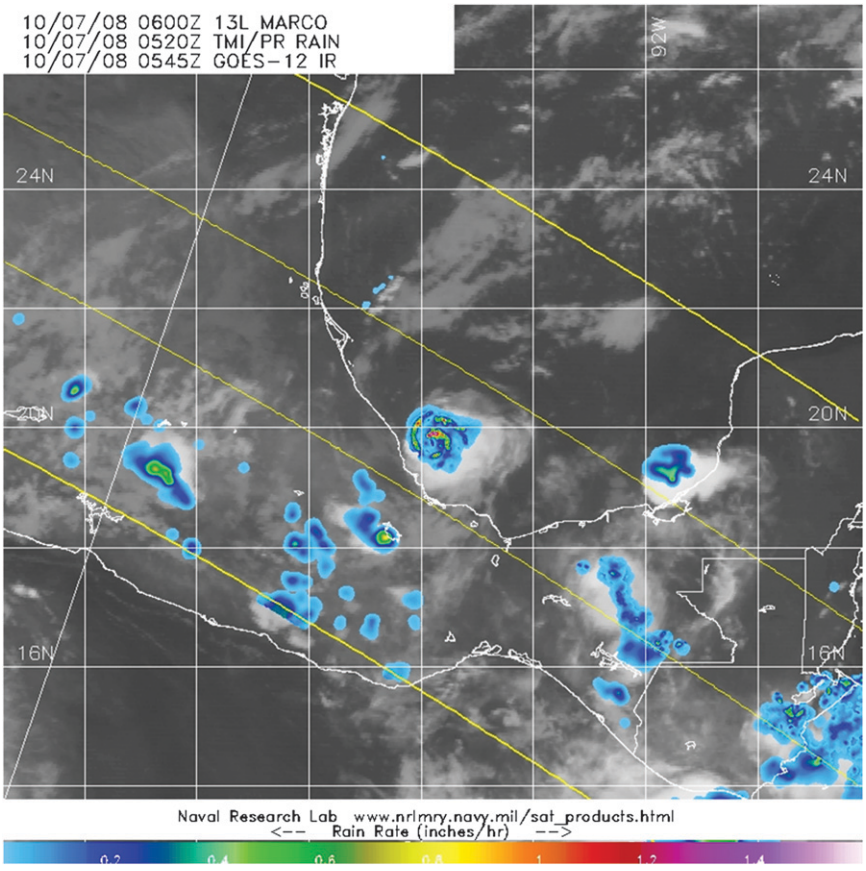

FIG. 8. Tropical Rainfall Measuring Mission (TRMM) Precipitation Radar depiction of rainfall rate associated with Marco at 0520 UTC 7 Oct 2008. Image obtained from Naval Research Laboratory (NRL) Marine Meteorology Division tropical cyclone page.

deep convection developed a couple of days later in the eastern Caribbean Sea. The convection continued to increase and became organized around the center during the next 36 h, and it is estimated that the system became a tropical depression around 0600 UTC 13 October, about 165 n mi south of the southeastern tip of the Dominican Republic. The westward movement of the depression slowed that day and the cyclone was slow to intensify after genesis, taking about 18 h to become a tropical storm, while centered about 125 n mi north-northeast of Aruba.

Omar moved slowly in a counterclockwise turn on 14 October, and this motion continued early the next day. Later on 15 October, the cyclone began moving toward the northeast under the influence of a broad, deep tropospheric trough to Omar's northwest and a mid- to low-level ridge to its east. This trough caused Omar to accelerate northeastward over the next few days, with the storm reaching a peak forward speed of about 30 kt on 17 October.

After becoming a tropical storm, a central dense overcast developed, and the cyclone underwent an extended period of rapid intensification. Omar's intensity increased from 35 kt at 0000 UTC 14 October to 115 kt at 0600 UTC 16 October. Omar reached hurricane intensity around 0000 UTC 15 October when it was centered about 115 n mi north of Bonaire.

The rapid intensification abruptly ended near 0600 UTC 16 October, and rapid weakening ensued, with Omar's maximum winds decreasing by 45 kt in 12 h. Microwave imagery around that time showed that the eye dissipated and the deep convection became well displaced to the north and east of an exposed low-level center (Fig. 9). This weakening appeared to be due to a combination of strong vertical wind shear and low- to midlevel dry air impacting the cyclone's inner core. Omar lost most of its deep convection by early on 17 October, and data from the Advanced Microwave Sounding Unit (AMSU) indicated that it had also lost its upper-level warm core.

Omar briefly reintensified later that day when the west-southwesterly vertical shear decreased while the hurricane still remained over warm waters. During this secondary peak in intensity, deep convection redeveloped around

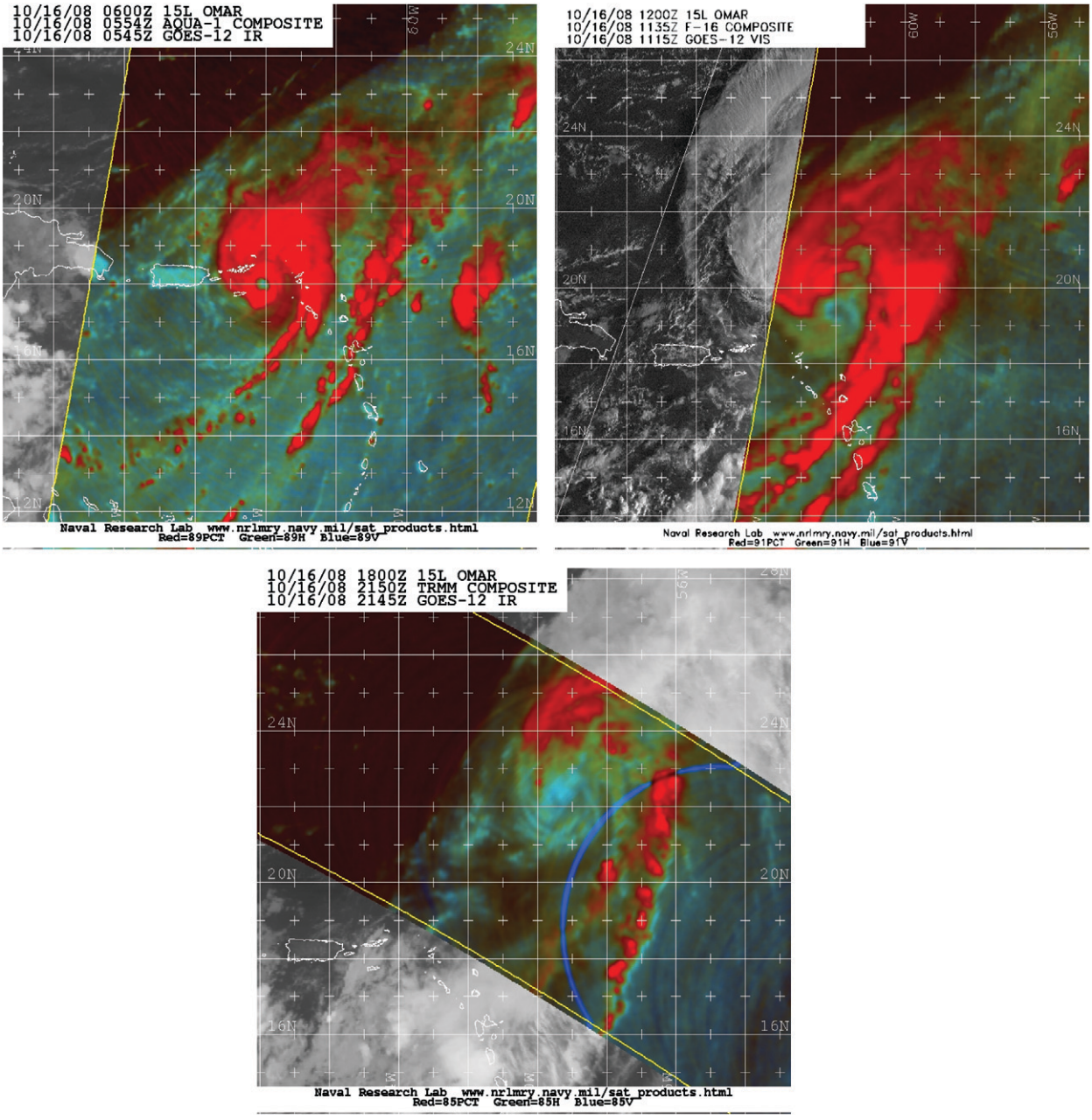

FIG. 9. Microwave imagery depicting the rapid demise of Omar's convective structure between 0554 and 2150 UTC 16 Oct 2008. Images courtesy of the NRL Marine Meteorology Division tropical cyclone page.

the center, and an eye was discernable for a few hours in both geostationary and microwave satellite imagery. Also on 17 October, the strong trough that had caused the rapid northeastward motion bypassed the hurricane. Omar decelerated, but continued moving toward the northeast and then the east-northeast during the next 3 days under the influence of a mid- to low-level ridge to its south and the midlatitude westerlies to its north.

Late on 17 October, westerly vertical shear again increased, and the hurricane moved over sea surface temperatures below 26°C, causing a final erosion of Omar's deep convection. The cyclone weakened to a tropical storm around 0000 UTC 18 October about 690 n mi east of Bermuda and then degenerated into a remnant low 12 h later. The low persisted for 2 days before dissipating around 0600 UTC 21 October about 700 n mi west of the Azores.

2) METEOROLOGICAL STATISTICS

Omar's peak intensity is estimated to be 115 kt at 0600 UTC 16 October; this estimate is based upon an SFMR wind observation of 113 kt, along with 700-mb flight-level winds of 132 kt.

Selected surface observations from land stations and data buoys are given in supplemental Table S9. The highest surface winds recorded were from St. Barthelemy, which reported a 1-min wind of 53 kt, and from the NOS station at Christiansted Harbor, St. Croix, which measured a 6-min mean wind of 52 kt. The peak observed gust was 75 kt from an unofficial site at the Buccaneer Resort at Christiansted, St. Croix.

Omar caused a storm surge in portions of the Virgin Islands and northern Leeward Islands. On Antigua, the surge was estimated at 0.60–1.10 m.

Storm total rainfall amounts of 50–150 mm were reported across the Virgin Islands and northern Leeward Islands, with a maximum of 231.9 mm at Antigua.

3) CASUALTY AND DAMAGE STATISTICS

There are no known casualties from Omar. At the time of its peak intensity, Omar was about 50 n mi west of Anguilla and St. Martin–St. Maarten in the Leeward Islands, and about 30 n mi southeast of Virgin Gorda in the British Virgin Islands. Fortunately, the center of Omar moved through the Anegada Passage, and the core of the major hurricane force winds did not impact any inhabited islands. Sombrero Island likely experienced the eye of Omar, but this island is uninhabited.

It is estimated that St. Thomas, in the U.S. Virgin Islands, received tropical storm conditions, while St. Croix—especially the eastern end of the island—was affected by category 1 hurricane conditions. In St. Croix, total damage was reported to be about $5 million (USD). There were no major impacts in the remaining U.S. Virgin Islands or in Puerto Rico.

The islands of Saba, St. Eustatius, and St. Maarten experienced tropical storm conditions and damaging coastal flooding. In Antigua, the storm surge caused flooding with water reaching near the roofs of some houses in low-lying areas. Large waves caused beach erosion and significant damage to coastal facilities in Aruba, Bonaire, and Curacao.

p. Hurricane Paloma, 5–9 November

1) SYNOPTIC HISTORY

Paloma originated from a broad area of disturbed weather that developed in the southwestern Caribbean Sea on 1 November. Convection in this region was intermittent for a couple of days but became more persistent on 4 November. The system continued to become better organized and it is estimated that a tropical depression formed around 1800 UTC 5 November, about 115 n mi southeast of the Nicaragua–Honduras border.

At the time of genesis, the depression was located on the southwestern edge of a mid- to upper-level ridge centered over the eastern Caribbean, resulting in an initial motion of the cyclone toward the northwest. The depression was situated in a small region of relatively low wind shear south of a belt of strong upper-level winds associated with a long-wave mid- to upper-level trough centered over the Gulf of Mexico. The combination of low shear and favorable oceanic conditions allowed the depression to intensify and become a tropical storm around 0600 UTC 6 November. Paloma then turned toward the north as it continued to move around the periphery of the ridge and reached hurricane strength around 0000 UTC 7 November, when it was centered about 155 n mi south-southwest of Grand Cayman.

Paloma began to intensify rapidly late on 7 November and became a major hurricane around 0000 UTC 8 November. Paloma reached its peak intensity of 125 kt (category 4) around 1200 UTC that day as it turned toward the northeast (Fig. 10a). During the 24-h period ending at 1200 UTC 8 November, Paloma's intensity increased by 50 kt. At its peak intensity, Paloma became the second strongest November Atlantic hurricane on record; only Hurricane Lenny (1999) was stronger (135 kt).[1] Paloma was a category 4 hurricane when the cyclone's eye passed just to the southeast of Little Cayman and Cayman Brac, with the northwestern eyewall passing over the eastern end of Cayman Brac.

Late on 8 November and early on 9 November, Paloma began to weaken when vertical wind shear increased markedly as the aforementioned mid- to upper-level trough continued to move eastward. As the hurricane approached Cuba, the strong upper-level southwesterly winds advected the mid- and upper-level portions of Paloma's circulation rapidly to the northeast (Fig. 10b). While weakening, the hurricane crossed the Jardines de la Reina Archipelago. Paloma is estimated to have been at category 3 strength when it impacted portions of those islands. The hurricane then made landfall on the main island of Cuba near Santa Cruz del Sur, Camagüey, Cuba; at that time Paloma is estimated to have been a category 2 hurricane, with maximum sustained winds of around 85 kt.

After landfall, the low-level center of Paloma continued northeastward for a short time, then slowed and

[1] This ranking is subject to revision based on potential adjustments to the best-track intensity of the November 1932 hurricane that also made landfall near Santa Cruz del Sur, Cuba.

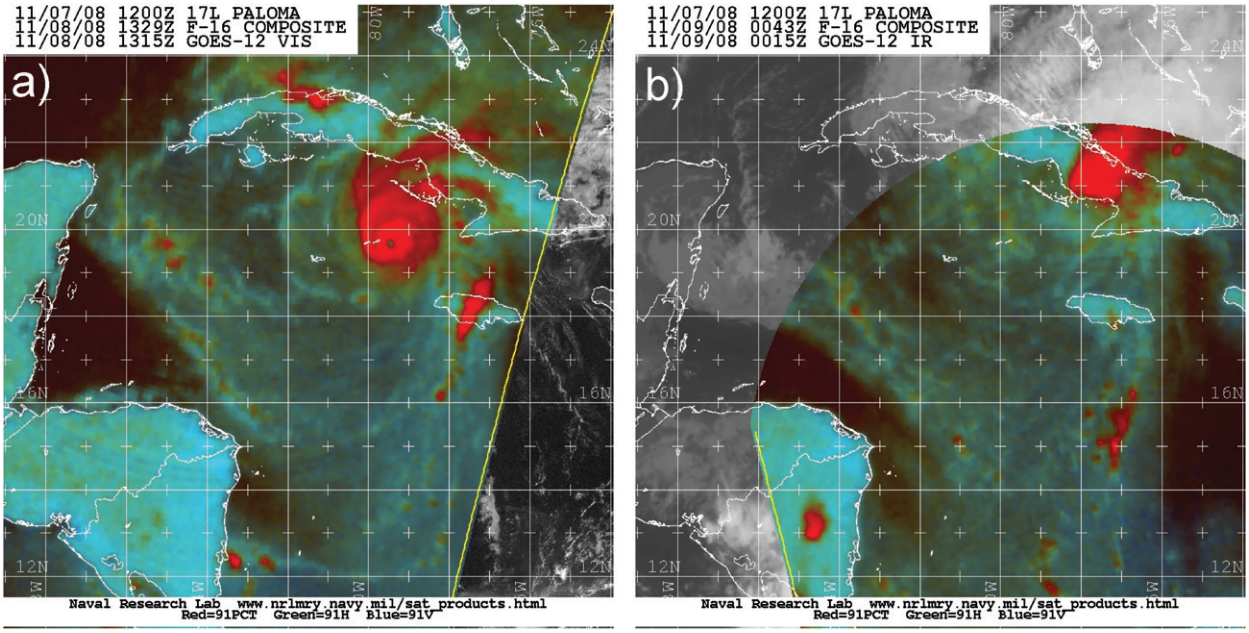

FIG. 10. Special Sensor Microwave Imager Sounder (SSMI/S) 91-GHz color composite image of Hurricane Paloma at (a) 1329 UTC 8 Nov 2008, near the time of the cyclone's maximum intensity and (b) 0043 UTC 9 Nov 2008, near the time of landfall in Cuba. Images courtesy of the NRL Marine Meteorology Division tropical cyclone page.

turned toward the northwest as it decoupled from the deep-layer flow. The cyclone weakened rapidly because of continued strong vertical wind shear, a decrease in deep convection, and interaction with the landmass of Cuba. Paloma became a tropical storm around 0600 UTC 9 November and further weakened to a tropical depression by 1800 UTC that day. During the 24-h period ending at 1200 UTC 9 November, Paloma is estimated to have weakened by 90 kt, from a 125-kt category 4 hurricane to a 35-kt tropical storm. By 0000 UTC 10 November, no deep convection was present near the circulation of Paloma, marking the degeneration of the cyclone into a remnant low.

On 10 November, the remnant low of Paloma moved slowly northward into the Atlantic waters just north of east-central Cuba, before becoming nearly stationary early on 11 November. Later that day, as a low-level ridge built to the north over the western Atlantic, Paloma's remnants began moving southwestward across Cuba before reentering the northwestern Caribbean Sea early on 12 November. The remnant low turned toward the west and west-northwest later that day, moved around the western periphery of the low-level ridge, and passed just north of the Isle of Youth around 0000 UTC 13 November before crossing the western tip of Cuba and entering the Gulf of Mexico. As Paloma's remnants accelerated northward, the surface low center became ill defined early on 14 November, about 60 n mi south-southwest of Apalachicola, Florida. Although the low-level center dissipated, moisture associated with the system contributed to the development of heavy rainfall in the Florida Panhandle later that day.

2) METEOROLOGICAL STATISTICS

The 125-kt estimated peak intensity of Paloma at 1200 UTC 8 November is based on a blend of a 127-kt wind measurement from the SFMR around 1110 UTC and a maximum flight-level wind of 134 kt measured at 0935 UTC, which corresponds to a surface intensity estimate of 121 kt using the standard 90% adjustment factor. This intensity was maintained at 1800 UTC based on a flight-level wind maximum of 142 kt at 1931 UTC, which equates to 128-kt intensity using the standard adjustment, and a wind measurement of 124 kt from the SFMR at 1935 UTC. Paloma began to weaken rapidly late on 8 November, as indicated by decreasing SFMR and flight-level wind measurements and a rising central pressure. The intensity at landfall is estimated to be 85 kt, based on a flight-level wind maximum of 94 kt measured around 2315 UTC 8 November, and an observed 78-kt sustained wind at 0130 UTC 9 November at Santa Cruz del Sur, Camagüey, Cuba (see supplemental Table S10).

On Cayman Brac, an unofficial anemometer at an elevation of 73 m above sea level measured a sustained wind of 131 kt (see supplemental Table S10) around

1200 UTC 8 November, near the time of Paloma's maximum intensity. On Grand Cayman, the highest reported sustained wind was 52 kt at the Owen Roberts International Airport on the western side of the island at 2206 UTC 7 November. On the eastern side of Grand Cayman, an automated station reported a maximum sustained wind of 50 kt.

In Cuba, the highest reported sustained wind was that previously mentioned at Santa Cruz del Sur, where a gust of 105 kt was also measured. Elsewhere in Camagüey, the highest reported sustained winds were between 34 and 39 kt, with gusts around 50 kt.

Paloma produced 451.4 mm of rain on Cayman Brac, with 153.7 mm reported on Grand Cayman. In Cuba, Paloma produced rainfall totals of 125–380 mm across portions of Camagüey, with maxima of 401.0 mm at Presa Najasa and 383.0 mm at Cuatro Caminos. In Las Tunas, rainfall of around 50–75 mm was reported.

A storm surge of 1.2–2.4 m is estimated to have occurred on Cayman Brac, with 0.6–1.2 m estimated on Little Cayman. No storm surge height estimates were received from Cuba; however, the Cuban Meteorological Service reported that storm surge penetrated inland 0.8 n mi in Santa Cruz del Sur and 0.4 n mi in Guayabal.

3) CASUALTY AND DAMAGE STATISTICS

No direct casualties or fatalities were reported in association with Paloma. The greatest impacts from Paloma occurred on Cayman Brac and Little Cayman. On Cayman Brac nearly every building on the island was damaged or destroyed, according to media reports from the Cayman Net News. Damage on Little Cayman was less severe, but trees and power lines along with some buildings were significantly damaged.

According to the government of Cuba, Paloma destroyed nearly 1500 homes and caused an estimated $300 million (USD) in damage on that island.

3. Tropical depressions that did not reach tropical storm strength

Tropical Depression Sixteen

Tropical Depression Sixteen formed from a broad area of low pressure over the southwestern Caribbean Sea. Convective activity became better organized around the low on 14 October, which led to the formation of a tropical depression around 1200 UTC that day, about 45 n mi northeast of the coast at the Nicaragua–Honduras border.

Convection near the center of the depression decreased somewhat that afternoon. The depression did not strengthen as it turned westward, then west-southwestward early on 15 October. The center of the poorly organized depression is estimated to have made landfall shortly after 1200 UTC 15 October along the northeast coast of Honduras, just west of Punta Patuca. The depression continued to move slowly west-southwestward, degenerating to a remnant low by 0000 UTC 16 October. A few hours later the low-level center dissipated over the mountains of east-central Honduras.

The depression and its remnants produced locally heavy rainfall over portions of Nicaragua, Honduras, eastern Guatemala, and Belize. Between 14 and 19 October, numerous locations in Honduras received more than 178 mm of rain, with a maximum amount of 360.4 mm on Roatan Island. In Belize, several locations received 250–500 mm of rain between 13 and 20 October with a maximum amount of 546.6 mm at Baldy Beacon.

Nine deaths in Central America are directly attributed to the depression. An Agence France-Presse (AFP) media report from 19 October indicates that 16 people lost their lives because of flooding from heavy rains produced in part by Tropical Depression Sixteen. The media report lists seven deaths in Costa Rica, four in Nicaragua, three in Honduras, and one each in El Salvador and Guatemala. However, the deaths in Costa Rica were likely the result of flooding rainfall that occurred before the depression formed.

4. Forecast verifications and warnings

The NHC verifies its tropical cyclone track and intensity forecasts by comparing the projected positions and intensities to the corresponding best-track positions and intensities for each cyclone derived from a poststorm analysis. Track forecast error is defined as the great-circle distance between a cyclone's forecast position and the best-track position at the forecast verification time. Forecast intensity error is defined as the absolute value of the difference between the forecast and best-track intensity at the forecast verifying time. Forecast skill, on the other hand, represents a normalization of the forecast errors against some standard or baseline. For track forecasts, skill is determined by comparing the official forecast errors with the error from the Climatology and Persistence model (CLIPER5; Neumann 1972; Aberson 1998). Intensity forecast skill is assessed using Decay-Statistical Hurricane Intensity Forecast (DSHIFOR5) as the baseline (Knaff et al. 2003; DeMaria et al. 2006). The DSHIFOR5 forecast is obtained by initially running SHIFOR5, the climatology and persistence model for intensity that is analogous to the CLIPER5 model for track (Jarvinen and Neuman 1979). The output from SHIFOR5 is then adjusted for land interaction by applying the decay rate of DeMaria et al. (2006).

TABLE 2. Homogenous comparison of official and CLIPER5 track forecast errors in the Atlantic basin for the 2008 season for all tropical and subtropical cyclones. Averages for the previous 5-yr period are shown for comparison.

	Forecast period (h)						
	12	24	36	48	72	96	120
2008 mean OFCL error (n mi)	27.7	48.3	68.6	88.2	126.9	159.8	191.8
2008 mean CLIPER5 error (n mi)	44.9	98.7	165.8	235.2	349.1	448.3	536.2
2008 mean OFCL skill relative to CLIPER5 (%)	38	51	59	63	64	64	64
2008 mean OFCL bias vector	281/6	279/13	277/22	279/30	265/37	284/22	355/33
2008 No. of cases	346	318	288	261	221	177	149
2003–07 mean OFCL error (n mi)	34.0	58.2	82.2	106.2	154.2	207.5	272.5
2003–07 mean CLIPER5 error (n mi)	46.6	96.6	152.6	205.9	301.0	393.1	480.2
2003–07 mean OFCL skill relative to CLIPER5 (%)	27	40	46	48	49	47	43
2003–07 mean OFCL bias vector [° (n mi)$^{-1}$]	307/7	312/15	316/23	320/32	317/33	328/29	001/38
2003–07 No. of cases	1742	1574	1407	1254	996	787	627
2008 OFCL error relative to 2003–07 mean (%)	−19	−17	−17	−17	−18	−23	−30
2008 CLIPER5 error relative to 2003–07 mean (%)	−4	2	9	14	16	14	12

Table 2 presents the results of the NHC official (OFCL) track forecast verification for the 2008 season, along with results averaged for the previous 5-yr period 2003–07. Mean track errors ranged from 28 n mi at 12 h to 192 n mi at 120 h. It is seen that mean official track forecast errors were smaller in 2008 than during the previous 5-yr period (by 17%–30%). The forecast projections at all lead times established new annual all-time lows. Over the past 15 yr or so, NHC has reduced its 24–72-h track forecast errors by about 50% (Franklin 2009). Vector biases were mostly westward (i.e., the official forecast tended to fall to the west of the verifying position) and were most pronounced at the middle forecast periods (e.g., about 30% of the mean error at 48 h). Track forecast skill in 2008 ranged from 38% at 12 h to 64% at 120 h (Table 2), and new records for skill also were set at all forecast lead times.

Table 3 presents the results of the NHC official intensity forecast verification for the 2008 season, along with results averaged for the preceding 5-yr period. Mean forecast errors in 2008 ranged from about 7 kt at 12 h to about 17 kt at 120 h. These errors were close to the 5-yr means through 48 h, and substantially below the 5-yr means after that. The 72–120-h intensity errors set records for accuracy. Forecast biases were small at all lead times. DSHIFOR5 errors were also below normal at 48 h and beyond. Given the challenges of forecasting rapid intensification, it is interesting and somewhat counterintuitive that this occurred in a year for which 9.1% of all 24-h intensity changes qualified as rapid strengthening, whereas during the period 2003–07, only 5.9% of all 24-h intensity changes qualified. The intensity error trend has shown virtually no net change during the past 15–20 yr and only a modest increase in skill has been achieved during that time (Franklin 2009).

Additional information on NHC's verification procedures, as well as a comprehensive evaluation of both

TABLE 3. Homogenous comparison of official and Decay-SHIFOR5 intensity forecast errors in the Atlantic basin for the 2008 season for all tropical and subtropical cyclones. Averages for the previous 5-yr period are shown for comparison.

	Forecast period (h)						
	12	24	36	48	72	96	120
2008 mean OFCL error (kt)	7.1	10.4	12.1	13.6	14.6	13.8	17.2
2008 mean Decay-SHIFOR5 error (kt)	8.7	12.4	14.7	15.6	16.9	17.7	18.9
2008 mean OFCL skill relative to Decay-SHIFOR5 (%)	18	16	17	12	13	22	8
2008 OFCL bias (kt)	0.4	1.3	1.6	2.2	3.1	1.6	1.3
2008 No. of cases	346	318	288	261	221	177	149
2003–07 mean OFCL error (kt)	6.7	10.0	12.3	14.3	18.2	19.7	21.8
2003–07 mean Decay-SHIFOR5 error (kt)	8.0	11.7	14.9	17.7	21.2	23.9	24.5
2003–07 mean OFCL skill relative to Decay-SHIFOR5 (%)	16	14	17	19	14	17	11
2003–07 OFCL bias (kt)	0.0	0.1	−0.5	−1.2	−2.2	−3.9	−4.8
2003–07 No. of cases	1742	1574	1407	1254	996	787	627
2008 OFCL error relative to 2003–07 mean (%)	6	4	−2	−5	−20	−30	−21
2008 Decay-SHIFOR5 error relative to 2003–07 mean (%)	9	6	−1	−11	−20	−26	−23

TABLE 4. Watch and warning lead times (defined as the time elapsed between the issuance of the watch or warning and the time of landfall or closest approach of the center to the coastline) for tropical cyclones affecting the United States in 2008. For cyclones with multiple landfalls, the most significant is given. If multiple watch or warning types (TS or H) were issued, the type corresponding to the most severe conditions experienced over land is given.

Storm	Landfall or point of closest approach	Watch type: Lead time (h)	Warning type: Lead time (h)
Cristobal	NC Outer Banks	None issued	TS: Conditions did not reach the coast
Dolly	South Padre Island, Texas	H: 51	H: 39
Edouard	McFaddin National Wildlife Refuge, Texas	TS: 39	TS: 27
Fay	Near Cape Romano, Florida	H: 48	TS: 24
Gustav	Cocodrie, Louisiana	H: 42	H: 30
Hanna	North Carolina/South Carolina border	H: 46	TS: 34
Ike	Galveston Island, Texas	H: 58	H: 40
Omar	U.S. Virgin Islands	H: 30	H: 24

official NHC forecasts and the objective guidance models, is given by Franklin (2009).

NHC defines a hurricane (or tropical storm) warning as a notice that 1-min mean winds of hurricane (or tropical storm) force are expected within a specified coastal area within the next 24 h. A watch indicates that those conditions are possible within 36 h. Table 4 lists lead times associated with those tropical cyclones that affected the United States in 2008. Because observations are generally inadequate to determine when hurricane or tropical storm conditions first reach the coastline, for purposes of this discussion lead time is defined as the time elapsed between the issuance of the watch or warning and the time of landfall or closest approach of the center to the coastline. Such a definition will usually overstate by a few hours the actual preparedness time available, particularly for tropical storm conditions. The table includes only the most significant (i.e., strongest) landfall for each cyclone, and only verifies the strongest conditions occurring on shore. Issuance of warnings for non-U.S. territories is the responsibility of the governments affected and is not tabulated here. The table shows that warning goals were met in 2008. Because of Ike's large size, significant storm surge was expected to impact the area well before the tropical storm–force winds reached the coast. Therefore, the hurricane watch and warning were issued earlier than normal.

Acknowledgments. The cyclone summaries are based on Tropical Cyclone Reports written by the authors and their NHC Hurricane Specialist colleagues: Lixion Avila, Robbie Berg, Jack Beven, Michael Brennan, Richard Pasch, Stacy Stewart, Todd Kimberlain, and Jamie Rhome. These reports are available online at http://www.nhc.noaa.gov/2008atlan.shtml. Ethan Gibney of the I. M. Systems Group at the NOAA/Coastal Services Center produced the track chart. Satellite images presented here were provided by David Stettner and Chris Velden of the University of Wisconsin—Madison Cooperative Institute for Meteorological Satellite Studies. Much of the local impact information contained in the individual storm summaries was provided by the meteorological services of the affected countries. In the United States, much of the local impact information is compiled by the local NWS Weather Offices. The National Data Buoy Center and the National Ocean Service provided summaries of data collected from their agencies.

REFERENCES

Aberson, S. D., 1998: Five-day tropical cyclone track forecasts in the North Atlantic basin. *Wea. Forecasting,* **13,** 1005–1015.

Blake, E. S., and R. J. Pasch, 2010: Eastern North Pacific hurricane season of 2008. *Mon. Wea. Rev.,* **138,** 705–721.

——, E. N. Rappaport, and C. W. Landsea, 2007: The deadliest, costliest, and most intense United States tropical cyclones from 1851 to 2006 (and other frequently requested hurricane facts). NOAA Tech. Memo. NWS TPC-5, 43 pp.

Bell, G. D., and Coauthors, 2000: Climate assessment for 1999. *Bull. Amer. Meteor. Soc.,* **81,** S1–S50.

——, E. Blake, S. B. Goldenberg, T. Kimberlain, C. W. Landsea, R. Pasch, and J. Schemm, 2009: Tropical cyclones—Atlantic basin: State of the climate in 2008. *Bull. Amer. Meteor. Soc.,* **90,** S79–S82.

Brennan, M. J., C. C. Hennon, and R. D. Knabb, 2009: The operational use of QuikSCAT ocean surface vector winds at the National Hurricane Center. *Wea. Forecasting,* **24,** 621–645.

DeMaria, M., J. A. Knaff, and J. Kaplan, 2006: On the decay of tropical cyclone winds crossing narrow landmasses. *J. Appl. Meteor. Climatol.,* **45,** 491–499.

Dvorak, V. E., 1984: Tropical cyclone intensity analysis using satellite data. NOAA Tech. Rep. NESDIS 11, National Oceanic and Atmospheric Administration, Washington, DC, 47 pp.

Franklin, J. L., 2009: 2008 National Hurricane Center forecast verification report. NOAA, 71 pp. [Available online at http://www.nhc.noaa.gov/verification/pdfs/Verification_2008.pdf.]

——, and D. P. Brown, 2008: Atlantic hurricane season of 2006. *Mon. Wea. Rev.,* **136,** 1174–1200.

——, M. L. Black, and K. Valde, 2003: GPS dropwindsonde wind profiles in hurricanes and their operational implications. *Wea. Forecasting,* **18,** 32–44.

Jarvinen, B. R., and C. J. Neuman, 1979: Statistical forecasts of tropical cyclone intensity for the North Atlantic basin. NOAA Tech. Memo. NWS NHC-10, 22 pp.

——, ——, and M. A. S. Davis, 1988: A tropical cyclone data tape for the North Atlantic basin. NOAA Tech. Memo. NWS NHC-22, 21 pp.

Kaplan, J., and M. DeMaria, 2003: Large-scale characteristics of rapidly intensifying tropical cyclones in the North Atlantic basin. *Wea. Forecasting,* **18,** 1093–1108.

Knaff, J. A., M. DeMaria, B. Sampson, and J. M. Gross, 2003: Statistical 5-day tropical cyclone intensity forecasts derived from climatology and persistence. *Wea. Forecasting,* **18,** 80–92.

Neumann, C. B., 1972: An alternate to the HURRAN (hurricane analog) tropical cyclone forecast system. NOAA Tech. Memo. NWS SR-62, 24 pp.

Office of the Federal Coordinator for Meteorology, 2008: National hurricane operations plan (NHOP). NOAA/OFCM, 188 pp. [Available online at http://www.ofcm.gov/nhop/08/nhop08.htm.]

Olander, T. L., and C. S. Velden, 2007: The Advanced Dvorak Technique: Continued development of an objective scheme to estimate tropical cyclone intensity using geostationary infrared satellite imagery. *Wea. Forecasting,* **22,** 287–298.

Rappaport, E. N., and Coauthors, 2009: Advances and challenges at the National Hurricane Center. *Wea. Forecasting,* **24,** 395–419.

Saffir, H. S., 1973: Hurricane wind and storm surge. *Military Eng.,* **423,** 4–5.

Simpson, R. H., 1974: The hurricane disaster potential scale. *Weatherwise,* **27,** 169–186.

Texas Tech University, 2006: A recommendation for an enhanced Fujita scale. 111 pp. [Available online at http://www.wind.ttu.edu/EFScale.pdf.]

Uhlhorn, E. W., P. G. Black, J. L. Franklin, M. Goodberlet, J. Carswell, and A. S. Goldstein, 2007: Hurricane surface wind measurements from an operational stepped frequency microwave radiometer. *Mon. Wea. Rev.,* **135,** 3070–3085.